Title

Neural Stem Cells Derived from Human Parthenogenetic Stem Cells Engraft and Promote Recovery in a Nonhuman Primate Model of Parkinson's Disease.

Journal

Cell transplantation, 25(11)

ISSN

0963-6897

Authors

Gonzalez, Rodolfo
Garitaonandia, Ibon
Poustovoitov, Maxim
et al.

Publication Date

2016-11-01

DOI

10.3727/096368916x691682

Peer reviewed

Cell Transplantation, Vol. 25, pp. 1945–1966, 2016

0963-6897/16 $90.00 + .00
DOI: http://dx.doi.org/10.3727/096368916X691682
E-ISSN 1555-3892
www.cognizantcommunication.com

Neural Stem Cells Derived From Human Parthenogenetic Stem Cells Engraft and Promote Recovery in a Nonhuman Primate Model of Parkinson's Disease

Rodolfo Gonzalez,*[1] Ibon Garitaonandia,*[1] Maxim Poustovoitov,* Tatiana Abramihina,* Caleb McEntire,† Ben Culp,† Jordan Attwood,† Alexander Noskov,* Trudy Christiansen-Weber,* Marwa Khater,‡ Sergio Mora-Castilla,‡ Cuong To,‡ Andrew Crain,§ Glenn Sherman,* Andrey Semechkin,* Louise C. Laurent,‡ John D. Elsworth,¶ John Sladek,# Evan Y. Snyder,§ D. Eugene Redmond Jr.,†¶ and Russell A. Kern*

*International Stem Cell Corporation, Carlsbad, CA, USA
†Axion Research Foundation, Hamden, CT, USA
‡Department of Reproductive Medicine, University of California San Diego, La Jolla, CA, USA
§Stem Cell Research Center, Sanford Burnham Prebys Medical Discovery Institute, La Jolla, CA, USA
¶Department of Psychiatry and Neurosurgery, Yale University School of Medicine, New Haven, CT, USA
#Department of Neurology, Pediatrics and Neuroscience, University of Colorado School of Medicine, Aurora, CO, USA

Cell therapy has attracted considerable interest as a promising therapeutic alternative for patients with Parkinson's disease (PD). Clinical studies have shown that grafted fetal neural tissue can achieve considerable biochemical and clinical improvements in PD. However, the source of fetal tissue grafts is limited and ethically controversial. Human parthenogenetic stem cells offer a good alternative because they are derived from unfertilized oocytes without destroying potentially viable human embryos and can be used to generate an unlimited supply of neural cells for transplantation. We have previously reported that human parthenogenetic stem cell-derived neural stem cells (hpNSCs) successfully engraft, survive long term, and increase brain dopamine (DA) levels in rodent and nonhuman primate models of PD. Here we report the results of a 12-month transplantation study of hpNSCs in 1-methyl-4-phenyl-1,2,3,6-tetrahydropyridine (MPTP)-lesioned African green monkeys with moderate to severe clinical parkinsonian symptoms. The hpNSCs manufactured under current good manufacturing practice (cGMP) conditions were injected bilaterally into the striatum and substantia nigra of immunosuppressed monkeys. Transplantation of hpNSCs was safe and well tolerated by the animals with no dyskinesia, tumors, ectopic tissue formation, or other test article-related serious adverse events. We observed that hpNSCs promoted behavioral recovery; increased striatal DA concentration, fiber innervation, and number of dopaminergic neurons; and induced the expression of genes and pathways downregulated in PD compared to vehicle control animals. These results provide further evidence for the clinical translation of hpNSCs and support the approval of the world's first pluripotent stem cell-based phase I/IIa study for the treatment of PD (Clinical Trial Identifier NCT02452723).

Key words: Parkinson's disease (PD); Neural stem cells (NSCs); Human parthenogenetic stem cells (hpSCs); Pluripotent stem cells; Cell therapy

INTRODUCTION

Parkinson's disease (PD) is a disorder characterized by a profound loss of function of the basal ganglia, which results from the loss of dopamine (DA) neurons in the substantia nigra pars compacta. Current therapeutic approaches for PD include the DA precursor, L-DOPA, and DA agonists, which increase DA function and provide meaningful clinical improvements for the initial years, but eventually patients experience diminished effects, shorter periods of benefit, and distressing side effects, such as hallucinations and severe dyskinesias[1]. In order to reduce the pharmacologically induced dyskinesias, a surgical approach known as

Received September 30, 2015; final acceptance August 10, 2016. Online prepub date: May 20, 2016.
[1]These authors provided equal contribution to this work.
Address correspondence to Dr. Russell A. Kern, International Stem Cell Corporation, 5950 Priestly Drive, Carlsbad, CA 92008, USA. Tel: +1-760-940-6383; Fax: +1-760-476-0600; E-mail: rk@intlstemcell.com

deep brain stimulation (DBS) was established[2,3]. DBS is a neuromodulatory treatment that provides symptomatic relief, especially of dyskinesias, for patients whose symptoms cannot be adequately controlled with medications[4]. Unfortunately, DBS loses efficacy after a few years, does not stop disease progression, and can lead to depression and the risk of suicide after surgery[5–8].

An alternative approach for the treatment of PD is cell-based therapy. Small open-label clinical trials have been conducted since the 1980s to evaluate the viability of administration of fetal neural cells into the striatum as a therapy for PD[9–24]. These first human studies demonstrated a wide variability of patient outcomes, with some exhibiting marked improvement. Transplantation of human fetal neural tissue into PD patients' brains was shown to provide clear neurological benefits[25–30], and in the best outcomes, the implanted cells survived, engrafted, connected to the host circuitry, released DA, and offered very long-term symptomatic benefit to PD patients sustained for up to 18 years without the need for pharmacological dopaminergic therapy[31,32]. Simultaneous transplantation of fetal tissue into the striatum and substantia nigra also led to an increase in the mean fluorodopa uptake in the putamen and substantia nigra, improvements in the total Unified Parkinson's Disease Rating Scale (UPDRS), and no intraoperative or perioperative complications[23].

After the encouraging evidence of the open-label studies, two double-blind placebo-controlled trials followed, but they did not reveal significant improvement over sham surgery[25,30]. However, when the groups were divided by age, younger patients (<60 years) or those with milder disease benefitted the most from the therapy, with the younger group showing a UPDRS improvement of 34% and a statistically significant difference in the undefined off scores versus the sham surgery group[25]. Some patients suffered from graft-induced dyskinesias, with three of them needing surgical intervention[25,30,33]. Unfortunately, fetal tissue is heterogeneous, clinically impractical, and ethically controversial. The difficulty of using several human fetal donors for each host has severely limited the number of effective transplantation procedures that can be carried out. Future cell replacement therapy in PD must rely on alternative tissue sources in which self-renewable stem cells can be propagated indefinitely in a standardized manner. Human pluripotent stem cells offer those qualities because they can be expanded indefinitely in the laboratory and provide an unlimited source of homogeneous cell populations for transplantation therapies. Neural cells derived from human pluripotent stem cell have been shown to ameliorate symptoms in preclinical models of PD[34–37].

In this study we used human parthenogenetic stem cells (hpSCs), which are pluripotent stem cells derived from chemically activated unfertilized oocytes[38,39]. hpSCs demonstrate the typical characteristics displayed by human embryonic stem cells (hESCs) including infinite division and in vitro and in vivo differentiation into cells of all three germ lineages[38,40,41] but avoid the ethical problem of destroying a potentially viable human embryo[38,40,41]. Additionally, human leukocyte antigen (HLA) homozygous hpSCs can be derived from both HLA homozygous or heterozygous donors with the potential to immune match a significant number of patients in cell-based therapy applications if the HLA type is common[39,42].

We have previously shown that hpSCs can be chemically directed to differentiate into a homogeneous population of multipotent neural stem cells (hpNSCs) that are scalable, cryopreservable, express all the appropriate neural markers, and can be further differentiated into functional dopaminergic neurons[43]. In a subsequent study, we showed that hpNSCs can functionally engraft and increase DA levels in two PD animal models: the 6-hyroxydopamine (6-OHDA)-lesioned rat and the DA-depleted asymptomatic 1-methyl-4-phenyl-1,2,3,6-tetrahydropyridine (MPTP)-lesioned African green monkey[44]. In this study, we evaluated the safety and efficacy over 12 months of two doses of Current Good Manufacturing Practice (cGMP)-manufactured hpNSCs (10^7 and 2×10^7 cells) injected in the striatum and substantia nigra of 18 MPTP-lesioned African green monkeys with moderate to severe PD symptoms. To study the biodistribution of the cells, two additional MPTP-lesioned monkeys were transplanted in the striatum with green fluorescent protein (GFP)- and red fluorescent protein (RFP)-labeled hpNSCs. Six monkeys were sacrificed at 6 months post-transplantation to evaluate the safety and tolerability at an intermediate time point, and an additional 12 monkeys were sacrificed at 12 months after administration to evaluate for therapeutic efficacy, reversibility, persistence, or late onset of toxicities, such as tumor formation or dyskinesia (Table 1). The experimental design was intended to determine whether monkeys treated with hpNSCs showed greater improvement than identically treated and randomly assigned control vehicle [Dulbecco's phosphate-buffered saline (DPBS)]-treated animals. The results of this study provide additional evidence for an hpNSC-based therapy and support the world's first pluripotent stem cell-based

Table 1. Study Design

Dose/Cells	No. of Monkeys	Sacrifices 6 Months	Sacrifices 12 Months
Vehicle control	6	1M, 1F	2M, 2F
Low cell dose 10^7	6	1M, 1F	2M, 2F
High cell dose 2×10^7	6	2M	1M, 2F

M, male; F, female.

therapy for PD. This is a single-arm, open-label, dose-escalating, phase I/IIa study evaluating the safety and tolerability of hpNSCs injected into the striatum and substantia nigra of patients with PD (Clinical Trial Identifier NCT02452723).

MATERIALS AND METHODS

Manufacturing of cGMP-Grade Human Parthenogenetic-Derived Neural Stem Cells

hpSC line LLC2P (International Stem Cell Corporation, Carlsbad, CA, USA)[38] was initially cultured under cGMP conditions in knockout Dulbecco's modified Eagle's medium (KDMEM)/F12 supplemented with 15% knockout serum replacement (KSR), 2 mM GlutaMAX, 0.1 mM minimum essential medium (MEM) nonessential amino acids, 0.1 mM β-mercaptoethanol, and 5 ng/ml basic fibroblast growth factor (bFGF) (all from Thermo Fisher Scientific, Carlsbad, CA, USA) on human neonatal skin fibroblasts (International Stem Cell Corporation) with mechanical passaging to preserve the genetic integrity of hpSCs[45,46]. The cells were then transferred to feeder-free and xeno-free conditions in Essential 8 Medium (Thermo Fisher Scientific) on CTS CELLstart substrate (Thermo Fisher Scientific) and subcultured with StemPro Accutase (Thermo Fisher Scientific) for three passages before neural induction. Then when the culture reached 80% confluency, the hpSCs were neuralized by treating with 5 μM SB218078 and 1 μM DMH-1 (both from Tocris, Bristol, UK) in KDMEM/F12, 1× GlutaMax, 1× N2/B27 Supplement (Thermo Fisher Scientific) for 11 days. Neuralized hpSCs were dissociated with StemPro Accutase and Y-27632 dihydrochloride (Tocris) and plated on CTS CELLstart-coated dishes in StemPro NSC serum-free medium (SFM) (Thermo Fisher Scientific). hpNSCs were expanded and cryopreserved to generate master and working cell banks comprising more than 2 billion cells each. The banks were extensively tested for expression of neural markers, absence of expression of pluripotency markers, sterility, mycoplasma, karyotype, short tandem repeat analysis, in vitro assays for adventitious viral contaminants, in vivo assays for adventitious viruses, a comprehensive panel of human viruses by quantitative PCR/RT-PCR, ultrastructure cell morphology and viral detection by thin section transmission electron microscopy, and PCR-based reverse transcription assay for retrovirus detection.

Flow Cytometry Analysis

Samples were harvested with StemPro Accutase (Thermo Fisher Scientific), washed with DPBS (Thermo Fischer Scientific), and fixed with 4% paraformaldehyde (PFA; Affymetrix, Santa Clara, CA, USA) for 30 min at room temperature (RT). Cells were washed twice with DPBS and blocked for 1 h at RT with 0.3% Triton X-100 (Sigma-Aldrich, St. Louis, MO, USA), 5% normal donkey serum (EMD Millipore, Temecula, CA, USA), and 1% bovine serum albumin (BSA; Sigma-Aldrich) in DPBS. Cells were then incubated overnight at 4°C with primary antibody in 0.3% Triton X-100, 5% normal donkey serum, and 1% BSA in DPBS (Table 2). Cells were washed twice with DPBS and incubated for 1 h at RT with secondary antibody in 0.3% Triton X-100, 5% normal donkey serum, and 1% BSA in DPBS. The samples were run and analyzed on a Becton Dickinson C6 Accuri Cytometer (BD Biosciences, San Jose, CA, USA).

GFP and RFP Constructs

GFP- and RFP-labeled hpNSCs were generated with the pGreenZeo (GFP, Cat. #SR501va-1) and pRedZeo (RFP, Cat. #SR10046va-1) (System Biosciences, Mountain View, CA, USA) according to the manufacturer's instructions.

MPTP Neurotoxin Administration

The study was performed in compliance with the US Department of Agriculture's (USDA) Animal Welfare Act (9 CFR Parts 1, 2, and 3) and with approval of the

Table 2. Antibodies

Antigen	Catalog #	Dilution	Application	Manufacturer
MSI1	ab52865	1:300	ICC	Abcam
	561468	1:20	Flow cytometry	BD Biosciences
NES	ab6320	1:200	ICC	Abcam
	561231	1:20	Flow cytometry	BD Biosciences
SOX2	ab79351	1:100	ICC	Abcam
	53-9811-82	1:100	Flow cytometry	eBiosciences
TH	P60101-0	1:500	IHC	Pel-Freeze
OCT-4	561628	1:20	Flow cytometry	BD Biosciences
SSEA-4	561565	1:20	Flow cytometry	BD Biosciences
CopGFP	AB513	1:2500	IHC	Evrogen
RFP	ab62341	1:100	IHC	Abcam

Institutional Animal Care and Use Committee (IACUC) from Axion Research Foundation and St. Kitts Biomedical Research Foundation, which maintains an Animal Welfare Assurance statement with the National Institutes of Health (NIH; Bethesda, MD, USA) Office of Laboratory Animal Welfare and is accredited by the AAALAC. Green monkeys of St. Kitts origin (*Chlorocebus sabaeus*) were injected intramuscularly with the neurotoxin MPTP (Sigma-Aldrich), which induces bilateral degeneration of the nigrostriatal pathway. Because of the varied sensitivity to the MPTP, 40 monkeys were treated in order to select a sample of 18 moderate to severe parkinsonian monkeys for the study. MPTP doses of 2.15 mg/kg were administered over a 5-day period[47,48], and the 18 monkeys with the greatest severity were pseudorandomly (stratified randomization) matched into the three treatment groups: animals receiving vehicle control, low-dose (10^7) hpNSCs, and high-dose (2×10^7) hpNSCs. The monkeys' Parkscores were ranked from highest to lowest. Then each triad of monkeys, based on the ranks, was randomized into three groups. This ensures that the groups were perfectly matched but with treatment assignment randomized. Male and female animals were allocated to each equal-sized treatment group with assignment based on Parkinson's score at 4 weeks after MPTP treatment to achieve a balanced Parkinson's score in each group. There were no significant differences at baseline between the three groups. Two additional MPTP-lesioned monkeys were used for the transplantantion of GFP- and RFP-labeled hpNSCs.

Immunosuppression

Because the test model involves grafting across species, all monkeys received triple immunosuppression, which was achieved with cyclosporine (1 mg/kg/day), prednisone (approximately 4.5 mg/kg/day) (both from Sandimmune; Henry Schein Animal Health, Pittsburgh, PA, USA), and azathioprine (starting at 5 mg/kg/day reducing to 1 mg/kg/day) (Sigma-Aldrich) starting 1 day prior to implantation and continuing until necropsy.

Transplantation of hpNSCs

Cells or vehicle (DPBS) control solution was implanted into the brain approximately 4 months after MPTP lesion using standard stereotactic procedures and verified stereotactic coordinates. The anesthetized monkeys were carefully placed into Kopf primate stereotactic units, the scalp opened in the midline, and the muscles retracted using a periosteal elevator sufficient to expose the stereotaxic targets for the procedure. A special Kopf drill was used to drill small, 2-mm holes at the site of each entry point, using a diamond-covered spherical drill. The carrier was then changed to one carrying a 22-gauge needle attached to a 100-µl Hamilton syringe (Hamilton, Reno, NV, USA) mounted on a microinfusion pump (Stoelting, Wood Dale, IL, USA). The cells or vehicle (DPBS) control solution was backfilled into the syringe, and the needles were lowered into five sites bilaterally at stereotactic targets as measured from ear bar zero (Table 3). In the low-dose group, animals received a total of 10 million cells, with 5 million cells per hemisphere and 1 million cells per injection site: anterior caudate nucleus, posterior caudate nucleus, anterior putamen, posterior putamen, and substantia nigra. Animals of the high-dose group received a total of 20 million cells, with 10 million cells per hemisphere and 2 million cells per injection site. The two monkeys transplanted with GFP- and RFP-labeled cells received a total of 20 million cells, and 10^7 GFP-labeled hpNSCs were implanted into four sites of the right striatum (anterior caudate nucleus, posterior caudate nucleus, anterior putamen, and posterior putamen) and 10^7 RFP-labeled hpNSCs into four sites of the left striatum. Insertion was performed slowly, and vehicle control or cell suspension at 100,000 cells/µl was extruded at a maximum rate of 2 µl/min, for a total volume of 10 µl (low dose), 20 µl (high dose), or 25 µl (GFP and RFP)

Table 3. Stereotactic Coordinates

	Anterior Posterior (mm)	Lateral (mm)	Vertical (mm)
Male			
Anterior caudate nucleus	23.1	4.0	19.0
Posterior caudate nucleus	19.1	4.0	19.0
Anterior putamen	23.1	10.0	19.0
Posterior putamen	19.1	10.0	19.0
Substantia nigra	13.1	4.0	9.6
Female			
Anterior caudate nucleus	23.1	3.5	19.0
Posterior caudate nucleus	19.1	3.5	19.0
Anterior putamen	23.1	9.5	19.0
Posterior putamen	19.1	9.5	19.0
Substantia nigra	13.1	3.5	9.6

per injection site. A 2-min delay was performed before cannula withdrawal, which was done at a rate of 1 μm/min. After all the injections were complete, the incision was irrigated, and the muscle, subcutaneous layer, and skin were closed using standard surgical methods. The animals were removed from the stereotactic device and monitored continuously until vital signs were stable and the animals were awake.

Behavioral Analysis

The scoring and rating of the behavior and motor movements of each monkey individually occurred during two observation periods per day several times a week without knowledge of the experimental variables (blind). From these quantitative assessments of 29 behaviors, a parkinsonian summary score was derived, based on a previous principal component factor analysis[49]. The parkinsonian summary score (Parkscore) contains different behaviors scored from 0 to 5, with 0 being "normal" and 5 being "severely parkinsonian," as well as time-based counts of specifically defined behaviors[49]. The Parkscore was used to classify subjects by severity, based on their average parkinsonian score after treatment. This method is highly responsive to pharmacological changes in DA function and correlates highly with striatal DA concentrations postmortem[48,50]. A broad range of normal behaviors was also quantified to enable a "healthy behavior score" (similar to the activities of daily living of the UPDRS) and was obtained for each animal[51]. Interrater reliability was assessed once a week, and the observers achieved a coefficient of concordance (Kendall's) greater than 0.95 on all behaviors, eliminating observer "drift" or idiosyncrasy. In addition to this behavioral score, a dyskinesia rating scale was also carried out once weekly on each monkey. These measures in combination with routine examination of brain for pathology allow the detection of possible detrimental effects of the implants[48,51–55].

Body Weight and Food Consumption

Body weights were measured and recorded upon screening for study recruitment, at the time of baseline phlebotomies, monthly during the study, and immediately prior to sacrifice. Food and water consumption were observed daily, and inadequate intake was responded to by additional food and water or by nasogastric tube if necessary.

Clinical Pathology

The animals were fasted overnight prior to sample collections or surgery. Animals were anesthetized, and blood samples (2–10 ml total volume per time point) were taken from the femoral vein via a 20-gauge needle attached to a 12-ml syringe for hematology, coagulation, and clinical chemistry measures, before MPTP administration, before test article administration, and every 3 months during the study until necropsy.

Necropsy and Tissue Processing

Complete necropsy examinations were performed under procedures approved by a facility veterinarian (St. Kitts Biomedical Research Foundation, St. Kitts, West Indies). On the designated day, the monkeys were anesthetized and euthanized, followed by whole-body perfusion of ice-cold saline, brain removal, and examination by the veterinarian. Brains were sliced into 4-mm coronal sections, and tissue punches were removed from standardized locations in the caudate nucleus, putamen, and substantia nigra; placed in cryotubes; and frozen in liquid nitrogen as previously described[47,56]. After all tissue punches had been collected, brain slices were preserved by immersion into fixative solution [4% PFA in 0.1 M phosphate buffer (pH 7.4)] (Sigma-Aldrich) at 4°C for 20±2 h. The solution was then replaced with fresh fixative, and after 6 h, the brain slices were moved into 0.1 M phosphate buffer (pH 7.4) containing sodium azide solution (0.1%) (Sigma-Aldrich). The animals were examined carefully for external abnormalities including palpable masses, and a comprehensive necropsy tissue collection was performed along with organ weight recording. Appropriate organ weight ratios were calculated (relative to body and brain weights), paired organs were weighed separately, and all tissues were fixed in 10% neutral-buffered formalin (Sigma-Aldrich) for pathology analysis.

Dopamine Analysis

DA and its metabolite, homovanillic acid (HVA), were extracted from the tissue punches in different regions of the striatum, separated by high-performance liquid chromatography (HPLC) and quantified by electrochemical detection according to published methods[48,57]. Concentrations were corrected for protein content, measured by the Lowry method.

Immunohistochemistry

Brain blocks were cut using MultiBrain Technology (NeuroScience Associates, Knoxville, TN, USA) at a thickness of 40 μm in the coronal plane. For immunofluorescence, monkey brain sections were washed in Tris buffer [0.1 M Tris, 0.85% NaCl (Sigma-Aldrich), pH 7.5] for 5 min, then 15 min in wash buffer (0.1% Triton X-100 in Tris buffer), and 15 min in blocking buffer (2% BSA, 0.1% Triton X-100 in Tris buffer) (Sigma-Aldrich). Sections were incubated with primary antibody diluted in blocking buffer at RT overnight with shaking (Table 2). Sections were washed for 15 min in wash buffer and 15 min in blocking buffer, and incubated for 1 h at RT with secondary antibody diluted in blocking buffer. Sections were washed four times, and coverslips were

mounted on the slides with mounting medium containing 4′,6-diamidino-2-phenylindole (DAPI; Vectashield Laboratories, Burlingame, CA, USA).

For 3,3′-diaminobenzidine (DAB) staining, sections were washed in Tris buffer for 5 min and incubated for 30 min in 3% H_2O_2, 10% methanol (Sigma-Aldrich) in Tris buffer. The sections were then washed for 5 min in Tris buffer, 15 min in wash buffer, and 15 min in blocking buffer. Sections were incubated with primary antibody diluted in blocking buffer at RT overnight with shaking. Sections were washed for 15 min in wash buffer and 15 min in blocking buffer, and incubated for 1 h at RT with biotinylated secondary antibody diluted in blocking buffer. The avidin–biotin complex (ABC) solution was prepared using the Vectastain Elite Standard ABC Kit (Vectashield) and mixed for 30 min. Sections were washed for 15 min in wash buffer and 15 min in blocking buffer. Sections were then incubated for 1 h in avidin–biotin–horseradish peroxidase (HRP) complex (ABC solution) and washed twice for 15 min in Tris buffer. The sections were finally developed in DAB solution (Vectashield).

Stereological Analysis

Cell counts were estimated by uniform random sampling with the optical fractionator method[58,59] using the "Stereo Investigator" software (MBF Bioscience Inc., Williston, VT, USA). Four sections per animals were counted bilaterally, and the tissue was sampled with a 10× objective using dissector *X-Y-Z* dimensions of 200×200×28 μm, using 2-μm guard zones above and below the counting box. The sampling grid was adjusted so that 10% of the selected region was counted. Data were expressed as average ± standard error of the mean (SEM).

Optical Density

The tyrosine hydroxylase (TH) immunoreactivity was visualized using an Axio Imager M2 microscope (Zeiss) with 20× objective and the AxioCam MRc digital camera (Carl Zeiss Vision Inc., San Diego, CA, USA). The optical density (OD) of the TH^+ fibers in the striatum was analyzed in three sections per animal using ImageJ software (NIH; http://rsb.info.nih.gov/ij/). The OD was calibrated using built-in functions of the software (http://imagej.nih.gov/ij/docs/examples/calibration/). The TH^+ images were converted to 8-bit grayscale, without rescaling. The OD of the striatum was assessed in three areas: rostral, mid, and caudal.

RNAseq Library Construction

RNA was isolated from tissue punches from the vehicle control, hpNSC-transplanted animals, and a healthy monkey with no MPTP lesion or intracranial injection. The RNA was isolated with the miRVana miRNA Isolation Kit, using the manufacturer's protocol for total RNA isolation (Thermo Fisher Scientific). Total RNA was quantified using the Quant-iT RiboGreen RNA Assay Kit (Thermo Fisher Scientific), and RNA quality was evaluated using RNA6000 Nano Kit and BioAnalyzer 2100 (Agilent Technologies Inc., La Jolla, CA, USA). RNAseq libraries were constructed using the TruSeq Stranded Total RNA Library Prep Kit (Illumina, San Diego, CA, USA). Sequencing and mapping were performed as previously described[60]. An average of 30.5 million uniquely mapped reads were generated per sample.

RNAseq Data Preprocessing

Counts for each gene were quantified using the python script RPKMforgenes (Karolinska Institutet, Stockholm, Sweden) and annotated using human reference genome version Ensembl GRCh37 (National Center for Biotechnology Information, Bethesda, MD, USA). We note that we mapped to the human reference genome because there is no high-quality reference genome for the African green monkey available. The average uniquely mapped read percent for this dataset was 65.9% (range, 51.5%–71.5%), which is within the normal range for even human datasets. Genes without at least one sample with at least 10 reads were removed from the analysis. An initial principal component analysis visualization was performed, and two putamen samples were found not to cluster with the other putamen samples and also had low uniquely mapped read counts after processing through RPKMforgenes and so were removed. The count data for the remaining samples were normalized using the R (v.3.1.1) package DESeq2 (v.1.4.5)[61,62].

Statistical Analysis

For continuous endpoints, descriptive statistics consists of means, SEM, and group size for each treatment group and time period. For categorical endpoints, incidence counts for each treatment group and time period were determined. Between-group differences were determined by one-way analysis of variance (ANOVA). Spearman rank correlation analyses were calculated comparing the mean Parkinson's and healthy behavior scores from the last month before sacrifice with the DA concentration, TH density in the striatum, and number of TH^+ neurons in the substantia nigra. Least-squares linear regression analyses were run on behavioral observations of the individual animals using the general linear models function of the Statistical Analysis System (version 6.12 for Macintosh; SAS Institute, Cary, NC, USA) to predict the regressions of the Parkscores and healthy behavior score, with 95% confidence level of the regression and determination of the significance of the slopes at $p < 0.05$. The sum scores derived from factor analyses[49] were used for analysis of the behavioral effects, thereby utilizing all of the data. These slopes provide some basis, along with

descriptive statistics, of determining treatment success or failure in individual animals that can be correlated with biological outcome data from biochemistry and histological cell counts. Both Parkinson's and healthy behavior scores were analyzed in this fashion. Group analyses were also carried out using a two-factor ANOVA with repeated measures, testing the control group and each individual dose group as the random factor, with repeated measures being each month of the study before MPTP treatment, after MPTP treatment, and monthly after the cell implantations. If there were significant interactions between Group and Month, the interactions were decomposed into simple main effects. Post hoc tests for significant differences were carried out using Newman–Keuls test at $p < 0.05$.

For all differential expression analyses of the RNAseq data, one-way ANOVA with post hoc Tukey's honest significant difference (HSD) multiple comparison of mean

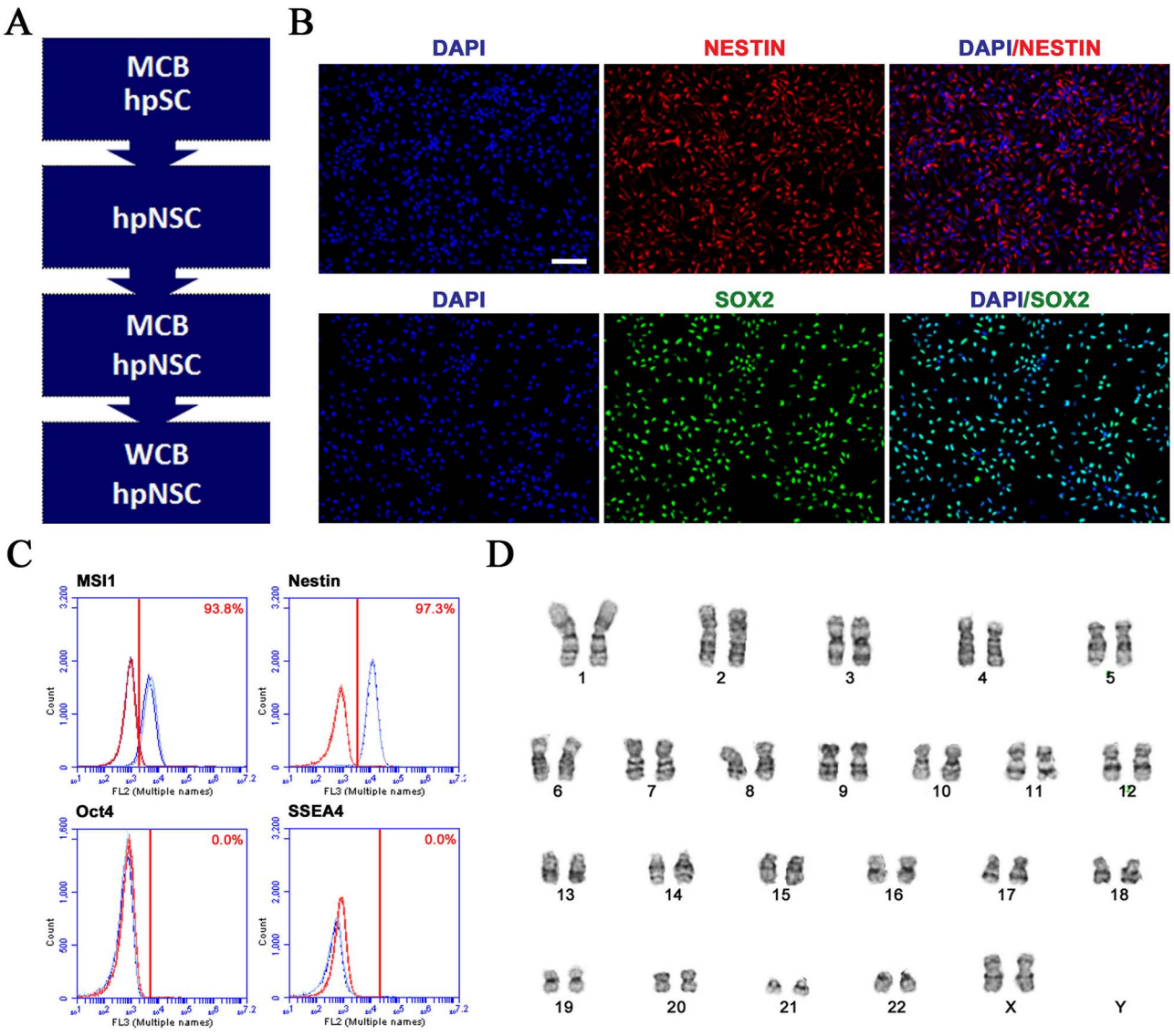

Figure 1. cGMP manufacturing and characterization of hpNSCs. (A) Schematic diagram showing the cGMP manufacturing process. First, a MCB of hpSCs is derived from unfertilized embryos. hpNSCs are then derived from hpSCs through a chemically directed differentiation method. The hpNSCs are then expanded into an MCB of hpNSCs. Finally, a vial of the MCB is expanded into a working cell bank (WCB) of hpNSCs. (B) Immunocytochemical analysis of hpNSCs shows that the cells are positive for neural markers SOX2 and nestin and have the appropriate morphology. Scale bar: 100 μm. (C) Quantitation by flow cytometry analysis of neural markers Musashi (MSI1) and nestin and pluripotency markers OCT-4 and SSEA-4. Representative flow cytometry data show that hpNSCs were more than 90% positive for neural makers and negative for pluripotency markers. Percentage of positive cells (blue) is calculated on the basis of isotype control-stained cells (red). (D) G-banding karyotyping analysis shows that the cells have a normal female 46 XX karyotype.

Table 4. Testing Results

Test	Result
In vitro assays for adventitious viral contaminants	Negative
In vivo assays for adventitious virus	Negative
Comprehensive panel of human viruses by quantitative PCR/RT-PCR	Negative
Ultrastructure cell morphology and viral detection by thin section transmission electron microscopy	Negative
Polymerase chain reaction (PCR)-based reverse transcription assay (PERT) for retrovirus detection	Negative
Mycoplasma (28 days)	Negative
Sterility (14 days)	Negative

for comparing different brain regions based on gene counts was performed. Multiple testing correction was performed according to Benjamini and Hochberg[63]. For comparisons between brain regions, cutoffs of values of $q \leq 0.001$ and fold change ≤ 0.67 or ≥ 1.5 were used. For comparisons between the hpNSC-transplanted and control animals, which were performed for each brain region separately, cutoffs of values of $q \leq 0.05$ and fold change ≤ 0.67 or ≥ 1.5 were applied. Functional enrichment analysis was performed using DAVID (National Cancer Institute, Frederick, MD, USA)[64,65]. Network analysis was performed using the GeneMANIA plugin[66,67] for Cytoscape[68,69] (US National Institute of General Medical Sciences, Bethesda, MD, USA). Other statistical analyses such as two-tailed Student's *t*-test, one-way ANOVA with Dunnett test, and two-way ANOVA with repeated measures were performed with GraphPad Prism (GraphPad Software Inc. La Jolla, CA, USA). The criterion for statistical significance under a confidence level of 95% ($\alpha = 0.05$) was $p < 0.05$.

RESULTS

Generation of cGMP-Grade hpNSCs for Transplantation

hpNSCs were derived from hpSCs through a chemically directed differentiation method as previously described[43,44]. Master and working cell banks of hpNSC were manufactured under cGMP conditions and tested throughout the manufacturing process (Fig. 1A). First, a master cell bank (MCB) of hpSCs was derived from unfertilized embryos under xeno-free conditions. Then hpNSCs were derived from hpSCs through a chemically directed differentiation method and expanded into an MCB of hpNSCs. Finally, a working cell bank (WCB) of hpNSCs was derived from a vial of MCB (Fig. 1A). Using flow cytometry analysis, hpNSCs were characterized by the expression of immature precursor markers such as nestin, Musashi, and (sex-determining region Y)-box 2 (Sox2) and the lack of pluripotent markers such as octamer-binding transcription factor 4 (OCT-4) and stage-specific embryonic antigen 4 (SSEA-4), which were used as release criteria to identify the hpNSCs that could promote recovery and qualify them for banking and testing (Fig. 1B and C). The hpNSCs were negative for mycoplasma and an extensive panel of adventitious agents as determined by in vitro, in vivo, and PCR-based assays and transmission electron microscopy (Table 4). hpNSCs passed the USP/EP-required sterility test without the growth of aerobic or anaerobic microorganisms (Table 4) and had a normal female 46 XX karyotype (Fig. 1D).

hpNSCs Promote Behavioral Recovery in PD Nonhuman Primates

The safety and efficacy of hpNSCs were assessed over a 12-month period in immunosuppressed *Chlorocebus sabaeus* monkeys with MPTP lesions and moderate to severe PD symptoms. The bilateral injection of 10^7 or 2×10^7 hpNSCs into the caudate nucleus, putamen, and substantia nigra was well tolerated by the MPTP parkinsonian monkeys. There were no deaths attributable to the cells, but one monkey died of an intracerebral hemorrhage. There were no test article-related serious adverse events in any of the monkeys at the 6- or 12-month time points. Body weight changes were similar between the groups (Fig. 2A), and hematology, coagulation parameters, and clinical chemistry differences were not noted between the groups at any of the time points. There were no apparent adverse behavioral or functional effects and no dyskinesia observed during the entire study.

All groups of monkeys improved after MPTP exposure, with decreasing Parkscores and increasing healthy behavior scores (Fig. 2B and C). The low cell dose group had the lowest Parkscores and highest healthy behavior scores at 12 months posttransplantation, but the difference with the control group was not statistically significant (Fig. 2B and C). Therefore, it was important to determine whether the treated groups improved significantly more than the control group over time. For this analysis, the scores of each group were compared before and 12 months posttransplantation and regressions were done separately for 12-month outcome periods by treatment group, and an analysis of covariance was done to determine whether the treatment groups were different from the controls (Fig. 2D–F). The Parkscore of the low-dose group at 12 months posttransplantation was significantly

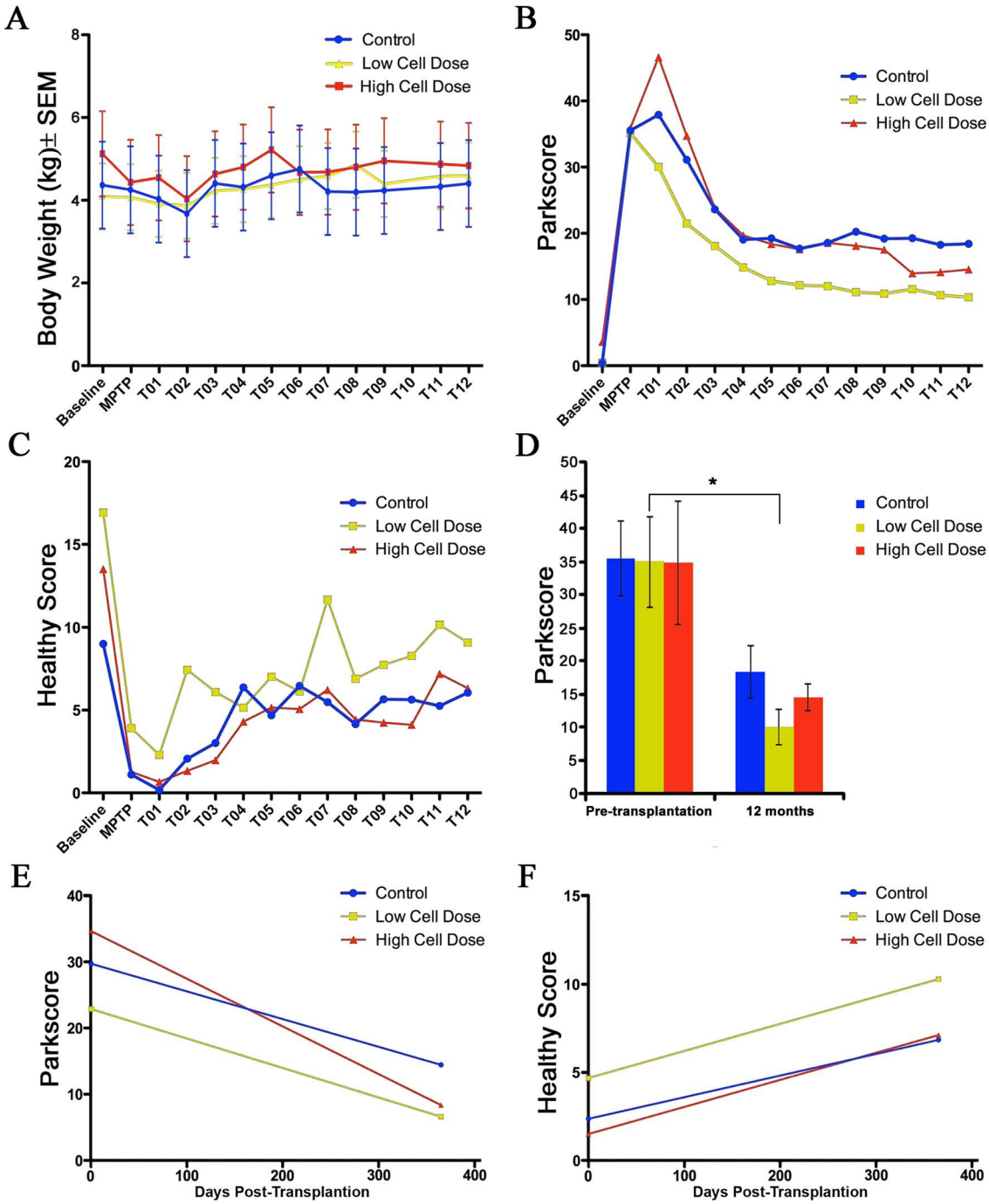

Figure 2. Behavioral recovery after hpNSC treatment. (A) Body weights throughout the 12-month study. Baseline: before MPTP lesion; MPTP: after MPTP lesion; T01–12: 1–12 months posttransplantation. (B, C) Treatment groups' Parkinson's score (B) and healthy behavior scores (C) for baseline, duration of MPTP exposure without treatment, and each month of life following treatment for animals that were sacrificed 12 months after injections. Parkinson's scores appeared to be lower for the low-dose group than for the controls, and both doses were lower than controls at the end, although this difference was not significant. The low-dose group also had higher healthy scores throughout most of the study; however, this also includes baseline and MPTP treatment before cell treatment, so it is hard to distinguish whether the higher scores are because of treatment effect or group effect ($n = 3$–4). (D) Comparison of Parkscores before and 12 months posttransplantation for all three groups. Only the low-dose group had significantly different Parkscores compared to baseline ($p < 0.0143$). (E, F) Predicted values of Parkscore (E) and healthy behavior score (F) for 12 months by treatment group. Only the postoperative period is shown. It is noteworthy that the low-dose group is different from the control group at 12 months (ANCOVA), and that the final scores of both the low-dose and the high-dose groups appear lower than the controls. The low-dose group also appears to show more healthy behaviors at 12 months, although this group began treatment with higher scores.

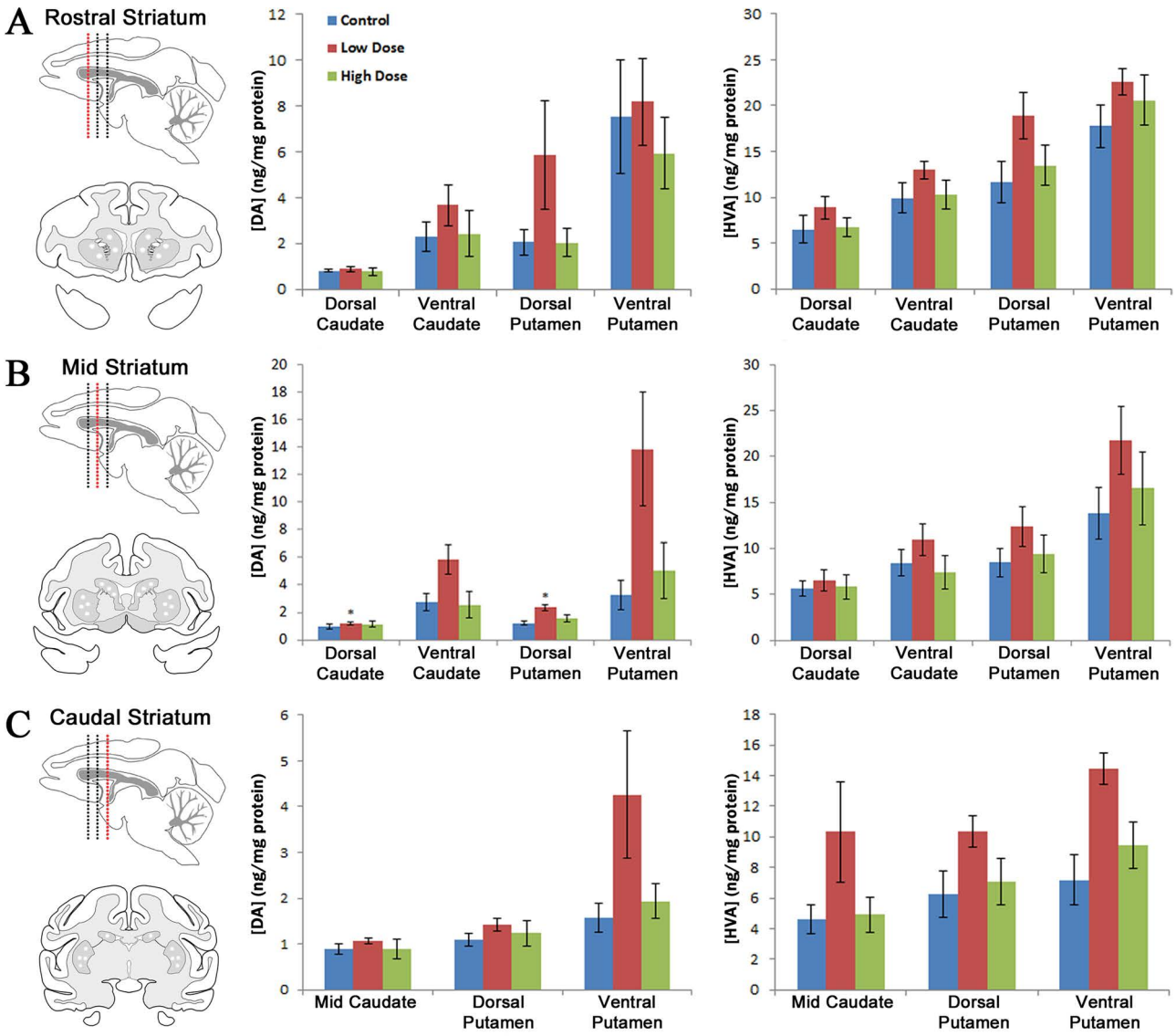

Figure 3. Biochemical changes after hpNSC treatment. On the left are schematics of parasagittal sections with a red dotted line indicating where the coronal diagram sections were taken. The coronal sections indicate where the punch biopsies were extracted from the caudate nucleus (CD) and putamen (PT) for the DA analysis in the rostral striatum (A), mid striatum (B), and caudal striatum (C). On the right are the concentrations of DA and HVA for each treatment group in the caudate nucleus and putamen. The low-dose group had consistently the highest DA and HVA concentrations in all the regions analyzed with statistically significant differences from vehicle control in the mid dorsal caudate nucleus and putamen (*$p<0.05$).

Table 5. Spearman Rank Correlations of Parkscore, Healthy Behavior Score, and DA levels

DA Levels	Parkscore	Healthy Behavior Score
Left hemisphere	$r=-0.9273$ ($p<0.0001$)	$r=0.7273$ ($p<0.01$)
Right hemisphere	$r=-0.9091$ ($p<0.0001$)	$r=0.8091$ ($p<0.0068$)
Mid ventral caudate	$r=-0.8364$ ($p<0.0023$)	$r=0.8000$ ($p<0.00466$)
Mid ventral putamen	$r=-0.9091$ ($p<0.00028$)	$r=0.7818$ ($p<0.0064$)

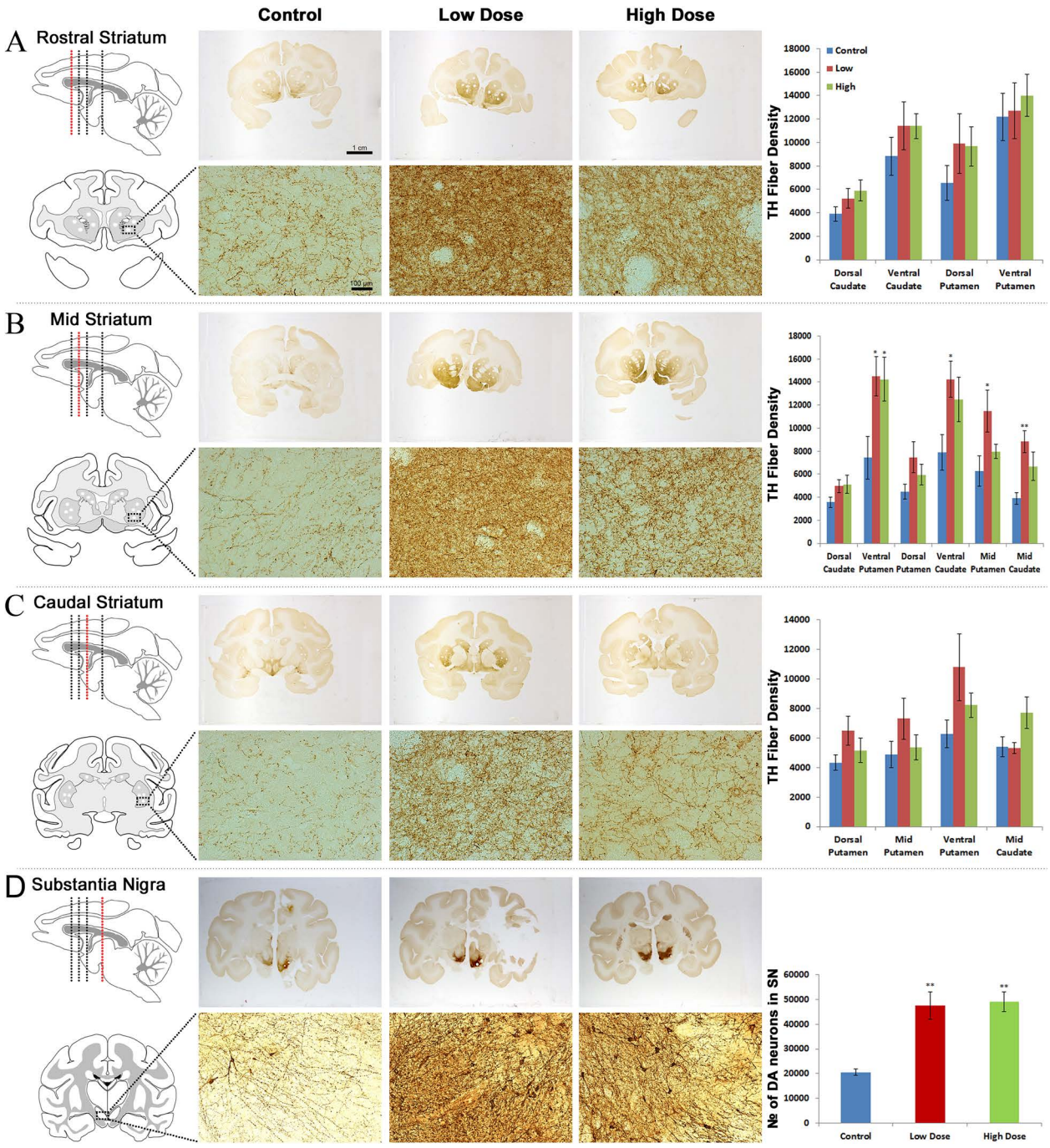

Figure 4. Histological analysis of nigrostriatal region at 12 months postimplantation. (A–C) Analysis of dopaminergic (TH^+) fiber density in the rostral (A), mid (B), and caudal (C) striatum. On the left, parasagittal diagrams with a red dotted line and coronal diagram with a dotted square indicating where the analysis was conducted. Center, representative coronal sections of the different regions of the striatum stained with TH (brown) from each treatment group and the micrographs taken from them. On the right, quantitation of the mean optical density measures of TH staining in the different regions of the striatum for all three groups. Treated groups had higher TH density in the rostral (A), mid (B), and caudal (C) striatum than control. In the mid striatum (C), which is close to the injection sites, the low-dose group had significantly higher TH density than the vehicle control in the ventral and mid caudate nucleus and putamen. (D) Quantitation of dopaminergic (TH^+) neurons in the substantia nigra. On the left, parasagittal section with red dotted line and coronal section with dotted square indicating where the analysis was conducted. Center, representative coronal sections of the substantia nigra stained with TH (brown) from each treatment group and the micrographs taken from them. On the right, quantitation of the number of TH^+ DA neurons in the substantia nigra for all three treatment groups. Both the low- and high-dose groups had significantly higher number of TH^+ DA neurons in the substantia nigra than the vehicle control animals ($^*p<0.05$, $^{**}p<0.01$).

Table 6. Spearman Rank Correlations of Parkscore, Healthy Behavior Score, Striatal DA levels, and TH Density

TH Density	Parkscore	Healthy Behavior Score	[DA] Mid Ventral Caudate	[DA] Mid Ventral Putamen
Mid ventral putamen	$r=-0.9000$ ($p<0.0004$)	$r=0.6636$ ($p<0.031$)	$r=0.7273$ ($p<0.0145$)	$r=0.9000$ ($p<0.00038$)
Mid ventral caudate	$r=-0.8818$ ($p<0.0007$)	$r=0.7818$ ($p<0.0064$)	$r=0.8636$ ($p<0.00116$)	$r=0.9545$ ($p<0.00002$)
Mid mid putamen	$r=-0.9545$ ($p<0.00003$)	$r=0.8000$ ($p<0.0047$)	$r=0.8091$ ($p<0.00395$)	$r=0.9364$ ($p<0.00008$)
Mid mid caudate	$r=-0.7909$ ($p<0.0055$)	$r=0.6364$ ($p<0.041$)	$r=0.8818$ ($p<0.0007$)	$r=0.9182$ ($p<0.0002$)
Caudal mid putamen	$r=-0.8000$ ($p<0.0047$)	$r=0.7636$ ($p<0.0086$)	$r=0.8818$ ($p<0.0007$)	$r=0.8182$ ($p<0.0033$)
Caudal ventral putamen	$r=-0.9000$ ($p<0.0004$)	$r=0.6182$ ($p<0.048$)	$r=0.7273$ ($p<0.0145$)	$r=0.8455$ ($p<0.00183$)
Rostral ventral caudate	$r=-0.7545$ ($p<0.0099$)	$r=0.7091$ ($p<0.0182$)	$r=0.6545$ ($p<0.0336$)	$r=0.7000$ ($p<0.0204$)
Rostral ventral putamen	$r=-0.7455$ ($p<0.0113$)	$r=0.7545$ ($p<0.0099$)	$r=0.6091$ ($p<0.0520$)	$r=0.6182$ ($p<0.0478$)

different ($p<0.0143$) from the score before transplantation, but this was not the case for the control and high-dose groups (Fig. 2D).

All three groups had almost identical Parkscores before transplantation, but the low-dose group showed a greater decrease in parkinsonism and the lowest scores at the end of 12 months (Fig. 2E and F). Analysis of covariance showed a statistically significant difference between the Parkscore slope of the low-dose and the control groups [$F(1, 1003)=6.21$, $p<0.02$] (Fig. 2E and F). There was no significant difference between the Parkscore slopes of the high-dose and control or the healthy behavior slopes of the low-dose and control groups (Fig. 2E and F). This test shows that the low-dose group was different from the control group, showing greater improvement in parkinsonism.

hpNSCs Promote Biochemical Changes in PD Nonhuman Primates

Postmortem, punch biopsies from the nigrostriatal region were analyzed for biochemical changes in DA and HVA to study the functional effects of the cells. Tissue punches were obtained from the dorsal and ventral areas of caudate nucleus and putamen, and the values for DA and HVA are shown in Figure 3. When the DA values from all the brain regions were combined, the low-dose group had the highest DA concentrations (5.81 ng/mg protein) versus the high-dose group (2.58 ng/mg protein) and the control (2.04 ng/mg protein), but the difference was not significant. However, when the values were analyzed separately by brain region, the largest differences between the low-dose and control groups were observed in the mid ventral regions and were statistically significant in the mid dorsal caudate nucleus ($p<0.0433$) and mid dorsal putamen ($p<0.0494$) (Fig. 3). DA turnover was analyzed by measuring the concentration of the DA metabolite, HVA, and the low-dose group had the highest HVA concentration in the mid striatum (Fig. 3). The low-dose group also had consistently higher DA and HVA levels in striatal areas rostral and caudal to the injection site (Fig. 3). There were no statistically significant differences between the two sides of the brain across all groups.

The overall relationship between the DA levels and the mean Parkscores and healthy behavior score in the final month of life of the monkeys was examined by Spearman rank correlations. Parkscore inversely correlated with DA levels on the left hemisphere ($r=-0.92727$; $p<0.0001$) and

FACING PAGE

Figure 5. Graphical representation of some of the most representative Spearman rank correlations between striatal TH density, Parkscore, healthy behavior score, and striatal DA levels. (A) Graphical representation of Spearman rank correlation between TH fiber density in the mid ventral putamen and Parkscore. (B) TH fiber density in mid mid putamen and Parkscore. (C) TH fiber density in mid ventral caudate and healthy behavior score. (D) TH fiber density in mid mid putamen and healthy behavior score. (E) TH fiber density in mid ventral caudate and DA concentration in the mid ventral putamen. (F) TH fiber density in mid mid putamen and DA concentration in the mid ventral putamen, (G) TH fiber density in mid mid caudate and DA concentration in mid ventral putamen. (H) TH fiber density in mid mid caudate and DA concentration in mid ventral caudate.

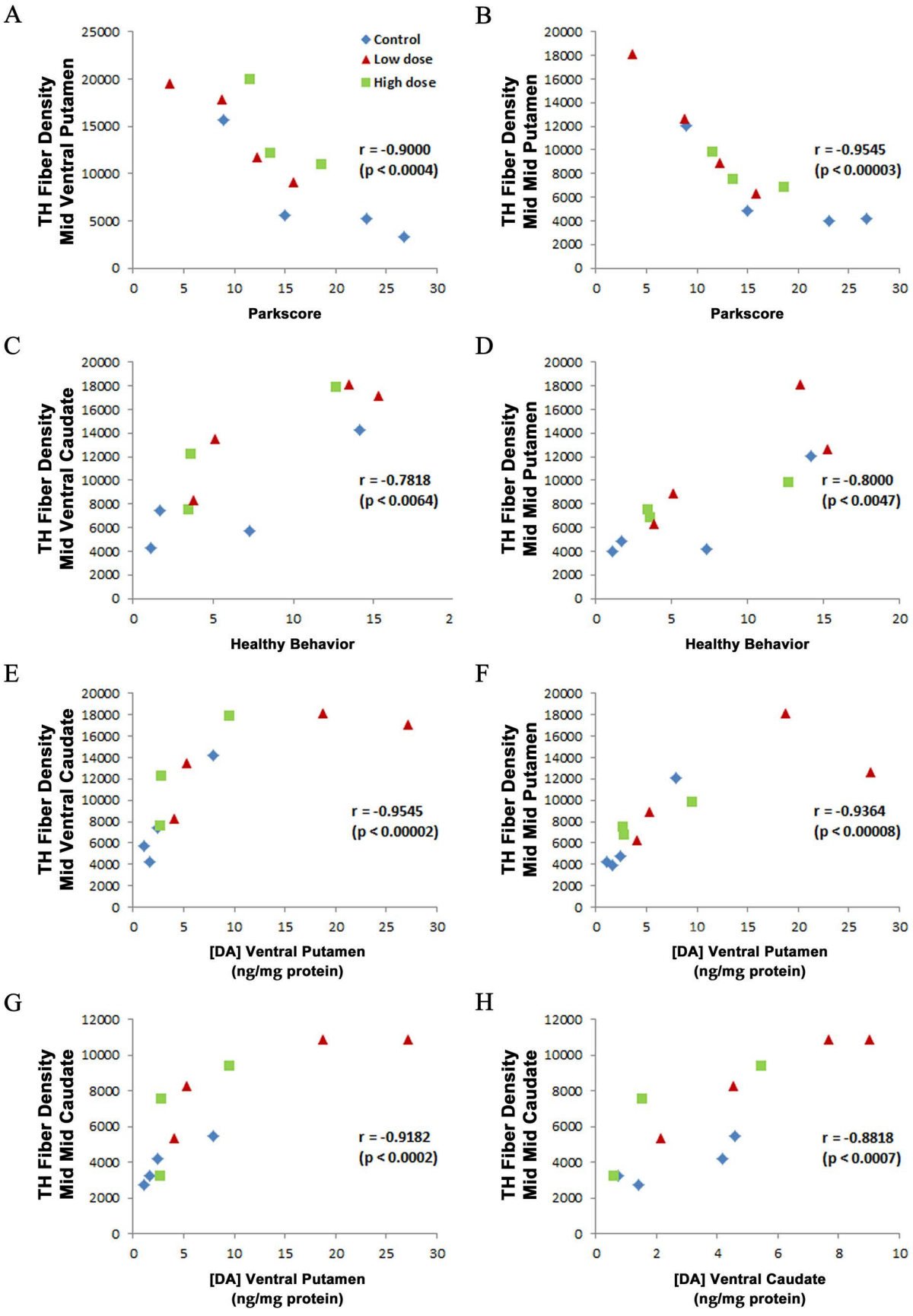
A
TH Fiber Density
Mid Ventral Putamen
Control
Low dose
High dose
r = -0.9000
(p < 0.0004)
Parkscore
B
TH Fiber Density
Mid Mid Putamen
r = -0.9545
(p < 0.00003)
Parkscore
C
TH Fiber Density
Mid Ventral Caudate
r = -0.7818
(p < 0.0064)
Healthy Behavior
D
TH Fiber Density
Mid Mid Putamen
r = -0.8000
(p < 0.0047)
Healthy Behavior
E
TH Fiber Density
Mid Ventral Caudate
r = -0.9545
(p < 0.00002)
[DA] Ventral Putamen
(ng/mg protein)
F
TH Fiber Density
Mid Mid Putamen
r = -0.9364
(p < 0.00008)
[DA] Ventral Putamen
(ng/mg protein)
G
TH Fiber Density
Mid Mid Caudate
r = -0.9182
(p < 0.0002)
[DA] Ventral Putamen
(ng/mg protein)
H
TH Fiber Density
Mid Mid Caudate
r = -0.8818
(p < 0.0007)
[DA] Ventral Caudate
(ng/mg protein)

on the right hemisphere ($r=-0.90909$; $p<0.0001$) (Table 5). There was also a positive correlation with healthy behavior and DA levels on the left hemisphere ($r=0.72727$; $p<0.01$) and on the right hemisphere ($r=0.80909$; $p<0.0068$) (Table 5). By region, Parkscore inversely correlated and health score positively correlated with DA levels in the mid ventral caudate and ventral putamen (Table 5).

hpNSCs Promote Host Dopaminergic Neuron Innervation and Recovery

Histological analysis of the brain tissue 12 months posttransplantation indicated higher dopaminergic neuron innervation in the striatum of monkeys transplanted with the low-dose cells (Fig. 4A–C). Coronal sections from the rostral, mid, and caudal striatum from all three groups were stained with TH, and the OD of the TH-stained fibers was measured in different regions of the caudate nucleus and putamen (Fig. 4A–C). The highest differences in fiber innervation between the low-dose group and the control were observed closer to the injection site in the mid striatum, with statistically significant differences in the mid ventral putamen ($p<0.018$), ventral caudate ($p<0.0308$), mid putamen ($p<0.0454$), and mid caudate ($p<0.0028$) (Fig. 4B). Even though the differences with control were not statistically significant in the rostral and caudal areas to the injection site, the low-dose group had consistently higher TH fiber innervation in all the regions examined. Additionally, stereological evaluation of the number of TH^+ neurons in the substantia nigra showed that both the low-dose group ($47{,}507 \pm 5{,}555$ cells) and high-dose group ($49{,}028 \pm 4{,}039$ cells) had a significantly higher number of DA neurons than the control group ($20{,}549 \pm 1{,}252$ cells) at 12 months posttransplantation (Fig. 4D).

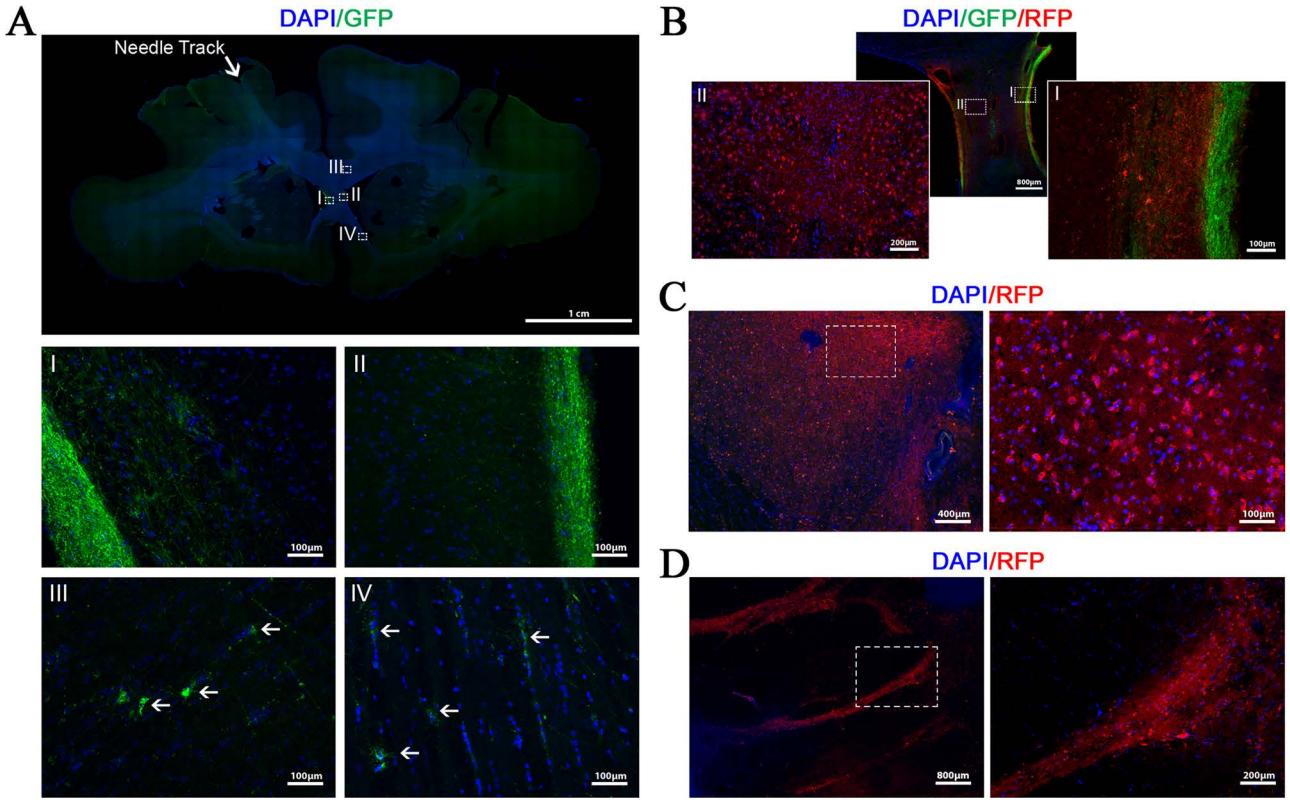

Figure 6. Survival, engraftment, and biodistribution of hpNSCs. (A) Coronal section of monkey striatum showing engraftment of GFP-labeled hpNSCs 12 months posttransplantation. The engrafted cells were detected with anti-GFP antibody (green). The numbered squares show the locations where the higher magnification micrographs were taken, and the white arrow points to the injection needle track. The first two micrographs (I, II) show the engrafted GFP-labeled cells lining the left (I) and right (II) lateral ventricle walls. The last two micrographs show GFP-labeled cells migrating in the corpus callosum (III) and septum pellucidum (IV). (B) GFP- and RFP-labeled cells lining the right and left lateral ventricle walls. The numbered rectangles show the locations where the higher magnification micrographs (I and II) were taken. RFP-labeled cells were detected with anti-RFP antibody (red). (C) Micrograph showing a graft of RFP-labeled cells in the ventral putamen. The dotted rectangle shows the location where the higher magnification micrograph on the right was taken. (D) RFP-labeled cells were found migrating through the internal capsule. The dotted rectangle shows the location where the higher magnification micrograph on the right was taken.

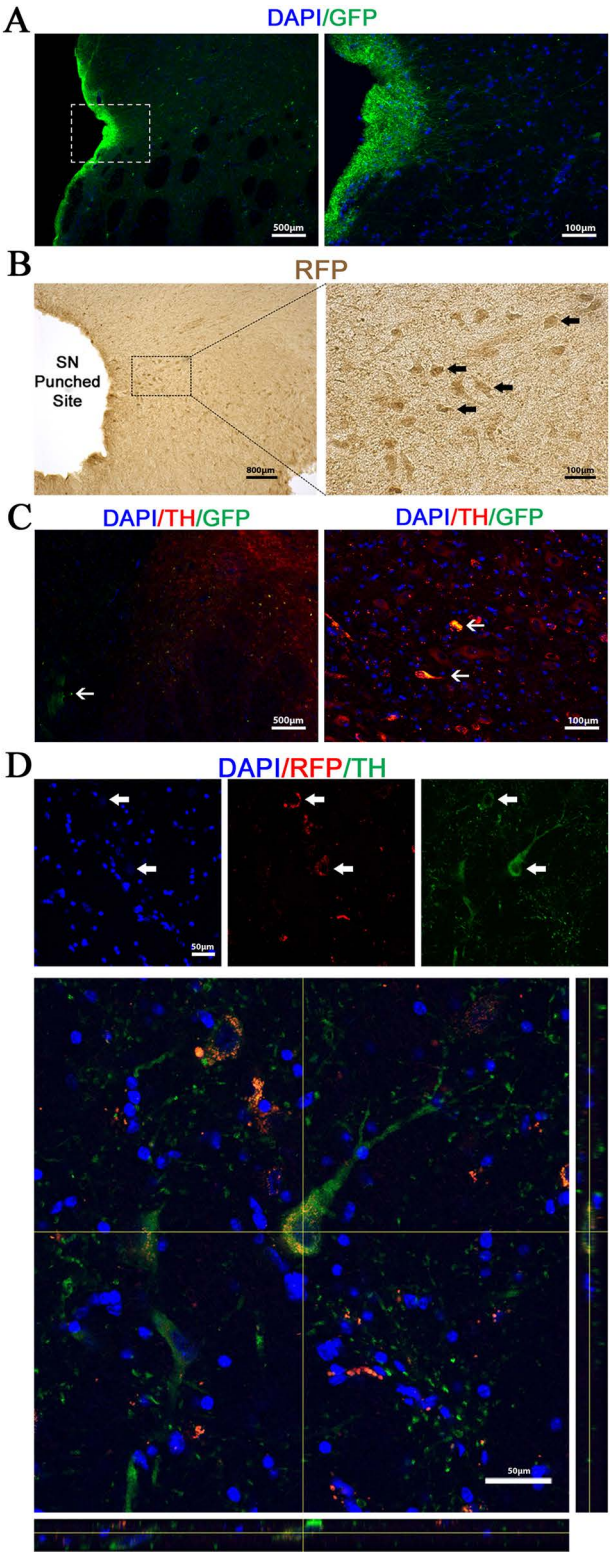

When the overall relationships between the TH fiber, DA levels, and the mean Parkscores and healthy behavior score in the final month of life of the monkeys were examined by Spearman rank correlations, it was observed that the Parkscore inversely correlated with TH fiber density in mid ventral putamen, mid ventral caudate, mid mid putamen, mid mid caudate, and caudal ventral putamen (Table 6 and Fig. 5). The healthy behavior score positively correlated with TH fiber density in the mid ventral caudate, mid mid putamen, caudal mid putamen, and rostral ventral putamen (Table 6 and Fig. 5). Striatal DA concentration in the ventral putamen and ventral caudate positively correlated with TH fiber density in the mid ventral caudate, mid mid putamen, and mid mid caudate (Table 6 and Fig. 5).

Biodistribution of hpNSCs

To track the biodistribution of the cells, a parallel experiment was run with two MPTP-lesioned monkeys transplanted with GFP-labeled hpNSCs in the left striatum and RFP-labeled cells in the right striatum. Survival and engraftment of the cells were confirmed 12 months posttransplantation by immunohistochemical analysis with anti-GFP and anti-RFP antibodies (Fig. 6). GFP- and RFP-labeled cells migrated extensively throughout the nigrostriatal pathway including the ventricles, corpus callosum, septum pellucidum, ventral tegmental area, and substantia nigra, including opposite hemispheres (Fig. 6). Figure 6A illustrates a coronal section of the striatum region showing the GFP-labeled cells (green) lining the left and right lateral ventricle walls and migrating through the corpus callosum and the septum pellucidum. Figure 6B shows GFP- and RFP-labeled cells lining both the right and left lateral ventrical walls, and Figure 6C shows an engrafted area of RFP-labeled cells in the ventral putamen. Transplanted cells were found migrating through the internal capsule (Fig. 6D) and all the way

FACING COLUMN

Figure 7. Migration of the hpNSCs to the substantia nigra region and in vivo differentiation into DA neurons. (A) GFP-labeled cells were found lining the side of the third ventricle next to the ventral tegmental area. The dotted rectangle shows the location where the higher magnification micrograph on the right was taken, which shows fiber innervation from the graft. (B) DAB staining of RFP-labeled cells showing their location in the substantia nigra close to the punched site. The dotted rectangle shows the location of the higher magnification image on the right, and the black arrows point to the RFP-labeled cells. (C) GFP-labeled graft (pointed by white arrow) located in the substantia nigra region close to the host TH^+ DA neurons (red). The micrograph on the right shows some GFP-labeled cells (green) colabeling with TH (red) and adopting dopaminergic phenotype (yellow, pointed by white arrows). (D) Confocal images showing RFP-labeled cells (red) in the substantia nigra colabeling with TH (green) (indicated by white arrows and yellow lines).

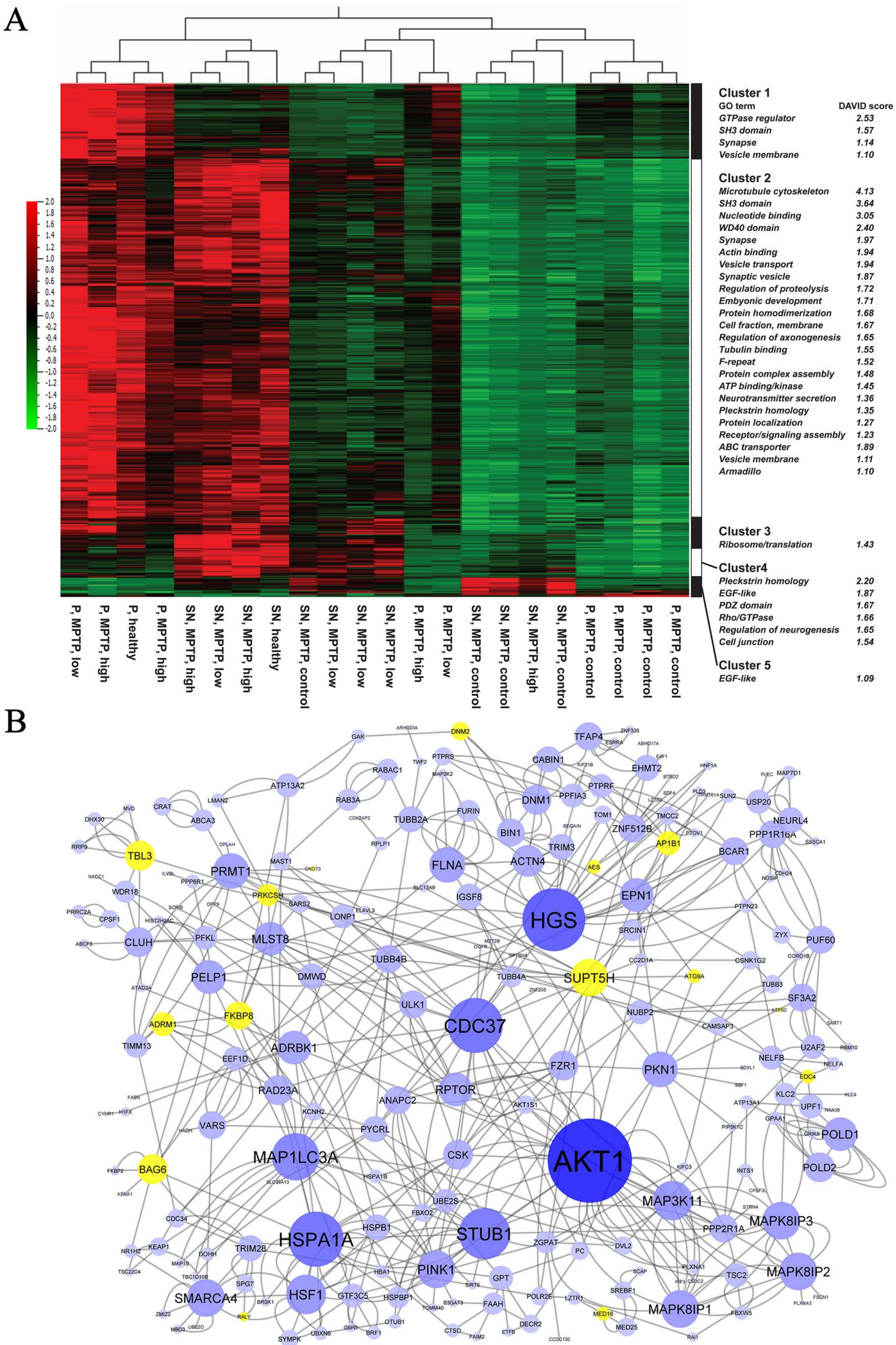
A
2.0
1.8
1.6
1.4
1.2
1.0
0.8
0.6
0.4
0.2
0.0
-0.2
-0.4
-0.6
-0.8
-1.0
-1.2
-1.4
-1.6
-1.8
-2.0
P, MPTP, low
P, MPTP, high
P, healthy
P, MPTP, high
SN, MPTP, high
SN, MPTP, low
SN, MPTP, high
SN, healthy
SN, MPTP, control
SN, MPTP, low
SN, MPTP, low
SN, MPTP, low
P, MPTP, high
P, MPTP, low
SN, MPTP, control
SN, MPTP, control
SN, MPTP, high
SN, MPTP, control
P, MPTP, control
P, MPTP, control
P, MPTP, control
P, MPTP, control
Cluster 1
GO term DAVID score
GTPase regulator 2.53
SH3 domain 1.57
Synapse 1.14
Vesicle membrane 1.10
Cluster 2
Microtubule cytoskeleton 4.13
SH3 domain 3.64
Nucleotide binding 3.05
WD40 domain 2.40
Synapse 1.97
Actin binding 1.94
Vesicle transport 1.94
Synaptic vesicle 1.87
Regulation of proteolysis 1.72
Embyonic development 1.71
Protein homodimerization 1.68
Cell fraction, membrane 1.67
Regulation of axonogenesis 1.65
Tubulin binding 1.55
F-repeat 1.52
Protein complex assembly 1.48
ATP binding/kinase 1.45
Neurotransmitter secretion 1.36
Pleckstrin homology 1.35
Protein localization 1.27
Receptor/signaling assembly 1.23
ABC transporter 1.89
Vesicle membrane 1.11
Armadillo 1.10
Cluster 3
Ribosome/translation 1.43
Cluster4
Pleckstrin homology 2.20
EGF-like 1.87
PDZ domain 1.67
Rho/GTPase 1.66
Regulation of neurogenesis 1.65
Cell junction 1.54
Cluster 5
EGF-like 1.09
B
AKT1
HGS
CDC37
HSPA1A
STUB1
MAP1LC3A
SUPT5H
TBL3
PRMT1
MLST8
PELP1
CLUH
FLNA
ACTN4
DNM1
BIN1
TRIM3
EPN1
ZNF512B
TFAP4
CABIN1
EHMT2
PTPRF
PPFIA3
AP1B1
BCAR1
PPP1R16A
USP20
NEURL4
PUF60
SF3A2
U2AF2
PKN1
FZR1
RPTOR
ANAPC2
ULK1
ADRBK1
RAD23A
VARS
PYCRL
CSK
MAP3K11
MAPK8IP3
MAPK8IP2
MAPK8IP1
PPP2R1A
POLD1
POLD2
TSC2
PINK1
HSF1
SMARCA4
TRIM28
HSPB1
GTF3C5
FAAH
GPT
ZGPAT
DVL2
BAG6
ADRM1
FKBP8
PRKCSH
TIMM13
WDR18
ATP13A2
RABAC1
RAB3A
TUBB2A
FURIN
IGSF8
LONP1
DMWD
TUBB4B
TUBB4A
SRCIN1
NUBP2
KLC2
UPF1
NELFB
DNM2
CRAT
ABCA3
PFKL
MAST1
SARS2
EEF1D

down to the substantia nigra region (Fig. 7A and B). Cell counts were performed in both hemispheres, and approximately 444,419 RFP-labeled cells were found in the putamen, 451,439 cells in the caudate, and 67,230 cells in the substantia nigra region. The total number of RFP-labeled cells engrafted in the nigrostriatal pathway was approximately 963,088, which accounts for 9.6% of the injected cells. Some of the engrafted GFP- and RFP-labeled cells in the substantia nigra colabeled with TH (Fig. 7B). Out of the 67,230 RFP-labeled cells found in the substantia nigra region, 17,820 cells were TH^+, which accounts for 1.85% of the total engrafted cells found in the nigrostriatal pathway.

Necropsy showed no evidence that the injection of the cells had any deleterious effect in any of the monkeys. Histopathological analysis by board-certified pathologists reported no microscopic evidence of tumor formation, ectopic tissues, or proliferative lesions in the brain or any of the tissues examined including lung, heart, liver, salivary glands, kidney, testis, ovary, thyroid, adrenal gland, pituitary, thymus, spleen, prostate, seminal vesicles, uterus, cerebrospinal fluid, cervical, thoracic, and lumbar spinal cord. Biodistribution analysis by qPCR did not detect the presence of the implanted cells in these tissues.

Gene Expression Analysis of Monkey Brains

We performed differential expression analysis among three brain regions separately (caudate, putamen, and substantia nigra) and analyzed the data to identify transcripts that were differentially expressed between control and hpNSC-transplanted animals (either low or high cell dose) (GEO dataset, GSE78921). No differentially expressed genes were detected for the caudate, while 549 genes were identified for the putamen and 325 for the substantia nigra, out of which 114 were more highly expressed in the hpNSC-transplanted animals for both the putamen and substantia nigra. We then performed hierarchical clustering of the transcripts that were differentially expressed between control and hpNSC-transplanted animals for these regions, which revealed five clusters of transcripts (Fig. 8A). After functional enrichment and network analyses of these clusters, we found the most interesting results for cluster 2, which was most highly expressed in the putamen and substantia nigra of three hpNSC-transplanted animals and a healthy animal (with no MPTP exposure or intracranial injection). Functional enrichment analysis of cluster 2 reveals enrichment of genes associated with many GO categories, including SH3 domain, WD40 domain, and synapse/vesicle transport/synaptic vesicle/neurotransmitter secretion. Cluster 2 contains PINK1 and ATP13A2, both of which have been associated with autosomal recessive hereditary parkinsonism. Network analysis (including physical interactions empirically demonstrated in humans and preclinical models) reveals five highly connected hubs (≥20 edges) (Fig. 8B). All but one of these hubs have been implicated in PD: AKT1 (37 edges)[70,71], HGS (26 edges), CDC37/HSP90 (22 edges)[72,73], STUB1/CHIP (20 edges)[74], and HSPA1A (22 edges)[75–77] (Fig. 7B).

DISCUSSION

In our study, we investigated the therapeutic potential of hpNSCs in a preclinical model of PD. Clinical-grade hpNSCs were manufactured and administered bilaterally into the striatum and substantia nigra of MPTP-lesioned African green monkeys with moderate to severe PD. The cells were injected into the striatum and substantia nigra because previous clinical studies by Mendez and colleagues showed that it can lead to significant improvement several years posttransplantation without complications[23,78,79]. The hpNSC-based therapy was well tolerated by the monkeys, and there were no test article-related serious adverse events such as tumors, ectopic tissue formation, or proliferative lesions in the brain or peripheral organs at the 6- or 12-month time points. The lack of tumors is one of the most critical parameters of a pluripotent stem cell-based therapy, attesting to the safety of this therapy[80]. There were no deaths attributable to the cells, but one monkey died of an intracerebral hemorrhage, a well-known risk of intracerebral injections, with some incidence in human studies using magnetic resonance imaging (MRI) guidance[81]. Monkeys showed no signs of dyskinesia during the entire study, which is a previously reported adverse event of the PD trials using fetal tissue[25,30]. There were no differences in body weight changes or clinical chemistry parameters between the groups. There were some

FACING PAGE

Figure 8. Hierarchical clustering for differentially expressed transcripts and network analysis of genes. (A) Hierarchical clustering for transcripts differentially expressed between control and hpNSC-transplanted animals for both substantia nigra and putamen. DAVID functional enrichment analysis results are shown for each cluster (DAVID score ≥1.10). (B) Network analysis of genes with higher expression in the substantia nigra and putamen of hpNSC-transplanted animals compared to controls. Genes from cluster 2 were subjected to network analysis using GeneMANIA. Blue nodes indicate genes that are differentially expressed between hpNSC-transplanted and control animals, while yellow nodes indicate genes (which are not differentially expressed) added by GeneMANIA to improve overall network connectivity. The connectedness of the genes was scored according to the number of physical interactions empirically demonstrated in humans and also predicted from interactions shown in preclinical models. More highly connected genes are indicated by circles that are both larger and have darker shading.

elevations in all groups in blood glucose levels, likely due to encouraging the monkeys to drink by added sugar to extra fluids.

All three groups of monkeys improved after MPTP exposure, with decreasing Parkscores and increasing healthy behavior scores. Even though the MPTP-lesioned African green monkey is the most comprehensive and studied preclinical PD model, it still has limitations and did not fully recapitulate in this case the disease progression characteristic in humans. The low cell dose group had the lowest Parkscores and highest healthy behavior scores at 12 months posttransplantation, but the difference with the control group was not statistically significant probably because of the spontaneous recovery previously observed by lesion-induced sprouting[49,82–85]. Although this study was large for a primate study, the number of animals in each group was relatively small, and larger effects might have been seen if there was greater statistical power. A longer outcome period might have also demonstrated continued improvement and divergence from the controls, as shown in human studies where clinical improvement peaked at 2 to 4 years posttransplantation[25,33]. We did observe however, a statistically significant difference between the Parkscore slope of the low-dose and the control groups by analysis of covariance. This difference was not observed for the high-dose group, which could have been due to a host rejection induced by the higher cell volume injected per site. Interestingly, Isacson's laboratory also observed that a lower dose of 10 million autologous iPSC-derived DA neurons outperformed a higher dose of 40 million cells in MPTP-lesioned nonhuman primates[86].

Biochemical analysis of striatal regions 12 months posttransplantation showed that the low-dose group had the highest DA and HVA concentrations, corresponding to lower parkinsonism[47,87]. Statistically significant differences between the low-dose group and the control group were observed in areas close to the injection sites, the mid dorsal caudate nucleus and mid dorsal putamen. The low-dose group also had consistently higher DA concentration and DA turnover in regions rostral and caudal to the injection site. There were no statistically significant differences between the two sides of the brain across all groups, but this was expected because the monkeys were given bilateral injections of the cells. We observed a high degree of correlation between the DA concentrations and Parkscores and healthy behavior scores, which is consistent with prior findings by Elsworth et al.[48,56] and Redmond Jr.[49] that, regardless of the cell treatment, there is a very high correlation between striatal DA concentrations and the Parkscore ratings.

Postmortem histological analysis of monkey brains showed that the low-dose group had significantly higher TH fiber density in striatal areas close to the injection sites than the control group. Even though the differences with control were not statistically significant in areas rostral and caudal to the injection sites, the TH fiber density was highest in the low-dose group in all the regions analyzed, consistent with the results from the Parkscores, healthy behavior scores, and biochemical measures. Spearman rank correlation analysis demonstrated that the TH fiber density in several striatal regions was highly correlated with Parkscore, healthy behavior score, and striatal DA concentrations. Stereological analysis showed that both the low- and high-dose groups had significantly higher number of TH^+ neurons in the substantia nigra than the control group. Coincidently, the low-dose group had over double the TH^+ neurons in the substantia nigra (~47,500 cells) and whole-brain DA concentration (5.81 ng/mg protein) than the control group (~20,500 cells and 2.04 ng/mg protein). The low-dose group had approximately 28.6% of the nigral DA neurons of unlesioned monkeys, whereas the control only had 12.3% of the DA neurons remaining[88]. According to Lindvall, a minimum of 100,000 DA neurons per putamen is necessary for successful transplantation of fetal transplants[89], which is roughly 25% of the total nigral DA neurons in a healthy individual[90] and similar to the percentage remaining in the low-dose group.

Further histological analysis showed clear evidence of survival and engraftment of the transplanted hpNSCs 12 months posttransplantation. We found the GFP- and RFP-labeled hpNSCs close to the injection sites in the striatum as well as evidence of their migration to areas including the ventricular system, corpus callosum, septum pellucidum, ventral tegmental area, and the substantia nigra. This degree of migration is consistent with previous reports utilizing human neural stem cells in nonhuman primates[54,91]. We found RFP-labeled cells migrating from the caudate to the putamen via the internal capsule and evidence of their migration to the opposite hemisphere via the corpus callosum. The approximate number of surviving cells in the nigrostriatal pathway of both hemispheres was 963,088 cells or 9.6% of the implanted RFP-labeled cells, out of which approximately 17,820 differentiated into DA neurons, or 1.85% of the total engrafted cells, which is consistent with previous reports indicating the in vivo differentiation of NSCs into DA neurons in the substantia nigra region[54,92]. The differentiation of hpNSCs into DA neurons in vivo accounts for most of the difference observed in nigral DA neurons between the control and hpNSC-transplanted samples (~27,000 DA neurons). The remaining DA neurons (~10,000 cells) are of host origin and could be accounted for by the neurotrophic support and neuroprotection provided by the implanted hpNSCs[44,54]. We previously showed that transplantation of hpNSCs in rodents led to significantly higher levels of the neuroprotective cytokines brain-derived neurotrophic

factor (BDNF) and glial cell line-derived neurotrophic factor (GDNF), which contributed to the significant increase in DA levels observed in these animals[44]. Additionally, results from differential expression analysis of RNAseq data suggest that hpNSCs induce expression of genes and pathways that have been previously reported to be downregulated in PD. The combined effects of neuroprotection, downregulation of PD-associated genes, migration, and cell replacement led to the overall higher number and innervation of DA neurons over control. As we observed from the fate analysis, a significant proportion of these DA neurons were of graft origin. In that sense, this therapy is similar to other hPSC-derived DA cell replacement approaches currently being developed[34,37,93,94], but differs in the fact that hpNSCs also migrate to the substantia nigra and provide neurotrophic support. There is a clinical trial currently being conducted in Europe known as the Transeuro trial, where fetal neural tissue is injected into PD patients, and results from this trial will also help in the development of future cell therapies[95].

In summary, this is the first comprehensive study showing functional recovery after transplantation of hpNSCs in a nonhuman primate with moderate to severe PD symptoms. The results of this and other studies support the clinical translation of hpNSCs and the approval of the world's first pluripotent stem cell-based therapy for treating PD.

ACKNOWLEDGMENTS: We thank the staff of St. Kitts Biomedical Research Foundation for care and observations of the monkeys. L.C.L., M.K., S.M.-C., and C.T. were supported by funds from the UCSD Department of Reproductive Medicine, and computation resources were provided through an allocation from XSEDE. R.G. and I.G.: conception and design, collection and/or assembly of data, data analysis and interpretation, article writing; M.P., T.A., C. M., B.C., J.A., A.N., T.C.-W., M.K., S.M.-C., C.T., A.C., G.S., A.S., L.C.L., J.D.E., J.S., E.Y.S.: collection and/or assembly of data; D.E.R. and R.K.: conception and design, data analysis and interpretation, article writing, final approval of the article. All authors who are employees of International Stem Cell Corporation declare stock option ownership. C.E., B.C., J.A., J.D.E., J.S., and D.E.R. are paid consultants of International Stem Cell Corporation. L.C.L. and E.Y.S. declare no conflicts of interest.

REFERENCES

1. Fahn S. Description of Parkinson's disease as a clinical syndrome. Ann N Y Acad Sci. 2003;991:1–14.
2. Limousin P, Pollak P, Benazzouz A, Hoffmann D, Le Bas JF, Broussolle E, Perret JE, Benabid AL. Effect of parkinsonian signs and symptoms of bilateral subthalamic nucleus stimulation. Lancet 1995;345(8942):91–5.
3. Siegfried J, Lippitz B. Bilateral chronic electrostimulation of ventroposterolateral pallidum: A new therapeutic approach for alleviating all parkinsonian symptoms. Neurosurgery 1994;35(6):1126–9; discussion 1129–30.
4. Alamri A, Ughratdar I, Samuel M, Ashkan K. Deep brain stimulation of the subthalamic nucleus in Parkinson's disease 2003–2013: Where are we another 10 years on? Br J Neurosurg. 2015;29(3):319–28.
5. Krack P, Batir A, Van Blercom N, Chabardes S, Fraix V, Ardouin C, Koudsie A, Limousin PD, Benazzouz A, LeBas JF, Benabid AL, Pollak P. Five-year follow-up of bilateral stimulation of the subthalamic nucleus in advanced Parkinson's disease. N Engl J Med. 2003;349(20):1925–34.
6. Ostergaard K, Aa Sunde N. Evolution of Parkinson's disease during 4 years of bilateral deep brain stimulation of the subthalamic nucleus. Mov Disord. 2006;21(5):624–31.
7. Rodriguez-Oroz MC, Obeso JA, Lang AE, Houeto JL, Pollak P, Rehncrona S, Kulisevsky J, Albanese A, Volkmann J, Hariz MI, Quinn NP, Speelman JD, Guridi J, Zamarbide I, Gironell A, Molet J, Pascual-Sedano B, Pidoux B, Bonnet AM, Agid Y, Xie J, Benabid AL, Lozano AM, Saint-Cyr J, Romito L, Contarino MF, Scerrati M, Fraix V, Van Blercom N. Bilateral deep brain stimulation in Parkinson's disease: A multicentre study with 4 years follow-up. Brain 2005;128(Pt 10):2240–9.
8. Voon V, Krack P, Lang AE, Lozano AM, Dujardin K, Schupbach M, D'Ambrosia J, Thobois S, Tamma F, Herzog J, Speelman JD, Samanta J, Kubu C, Rossignol H, Poon YY, Saint-Cyr JA, Ardouin C, Moro E. A multicentre study on suicide outcomes following subthalamic stimulation for Parkinson's disease. Brain 2008;131(Pt 10):2720–8.
9. Lindvall O, Brundin P, Widner H, Rehncrona S, Gustavii B, Frackowiak R, Leenders KL, Sawle G, Rothwell JC, Marsden CD, Bjorklund A. Grafts of fetal dopamine neurons survive and improve motor function in Parkinson's disease. Science 1990;247(4942):574–7.
10. Lindvall O, Rehncrona S, Brundin P, Gustavii B, Astedt B, Widner H, Lindholm T, Bjorklund A, Leenders KL, Rothwell JC, Frackowiak R, Marsden D, Johnels B, Steg G, Freedman R, Hoffer BJ, Seiger A, Bygdeman M, Stromberg I, Olson L. Human fetal dopamine neurons grafted into the striatum in two patients with severe Parkinson's disease. A detailed account of methodology and a 6-month follow-up. Arch Neurol. 1989;46(6):615–31.
11. Freed CR, Breeze RE, Rosenberg NL, Schneck SA, Wells TH, Barrett JN, Grafton ST, Huang SC, Eidelberg D, Rottenberg DA. Transplantation of human fetal dopamine cells for Parkinson's disease. Results at 1 year. Arch Neurol. 1990;47(5):505–12.
12. Henderson BT, Clough CG, Hughes RC, Hitchcock ER, Kenny BG. Implantation of human fetal ventral mesencephalon to the right caudate nucleus in advanced Parkinson's disease. Arch Neurol. 1991;48(8):822–7.
13. Lindvall O, Widner H, Rehncrona S, Brundin P, Odin P, Gustavii B, Frackowiak R, Leenders KL, Sawle G, Rothwell JC, Bjorklund A, Marsden CD. Transplantation of fetal dopamine neurons in Parkinson's disease: One-year clinical and neurophysiological observations in two patients with putaminal implants. Ann Neurol. 1992;31(2):155–65.
14. Widner H, Tetrud J, Rehncrona S, Snow B, Brundin P, Gustavii B, Bjorklund A, Lindvall O, Langston JW. Bilateral fetal mesencephalic grafting in two patients with parkinsonism induced by 1-methyl-4-phenyl-1,2,3,6-tetrahydropyridine (MPTP). N Engl J Med. 1992;327(22):1556–63.
15. Freed CR, Breeze RE, Rosenberg NL, Schneck SA, Kriek E, Qi JX, Lone T, Zhang YB, Snyder JA, Wells TH, Ramig LO, Thompson L, Mazziotta JC, Huang SC, Grafton ST, Brooks D, Sawle G, Schroter G, Ansari AA. Survival of implanted fetal dopamine cells and neurologic improvement 12 to 46 months after transplantation for Parkinson's disease. N Engl J Med. 1992;327(22):1549–55.

16. Spencer DD, Robbins RJ, Naftolin F, Marek KL, Vollmer T, Leranth C, Roth RH, Price LH, Gjedde A, Bunney BS, Sass KJ, Elsworth JD, Kier EL, Makuch R, Hoffer PB, Redmond DE Jr. Unilateral transplantation of human fetal mesencephalic tissue into the caudate nucleus of patients with Parkinson's disease. N Engl J Med. 1992;327(22):1541–8.
17. Peschanski M, Defer G, N'Guyen JP, Ricolfi F, Monfort JC, Remy P, Geny C, Samson Y, Hantraye P, Jeny R, Gaston A, Keravel Y, Degos JD, Cesaro P. Bilateral motor improvement and alteration of L-dopa effect in two patients with Parkinson's disease following intrastriatal transplantation of foetal ventral mesencephalon. Brain 1994;117 (Pt 3):487–99.
18. Lindvall O, Sawle G, Widner H, Rothwell JC, Bjorklund A, Brooks D, Brundin P, Frackowiak R, Marsden CD, Odin P, Rehncrona S. Evidence for long-term survival and function of dopaminergic grafts in progressive Parkinson's disease. Ann Neurol. 1994;35(2):172–80.
19. Defer GL, Geny C, Ricolfi F, Fenelon G, Monfort JC, Remy P, Villafane G, Jeny R, Samson Y, Keravel Y, Gaston A, Degos JD, Peschanski M, Cesaro P, Nguyen JP. Long-term outcome of unilaterally transplanted parkinsonian patients. I. Clinical approach. Brain 1996;119 (Pt 1):41–50.
20. Levivier M, Dethy S, Rodesch F, Peschanski M, Vandesteene A, David P, Wikler D, Goldman S, Claes T, Biver F, Liesnard C, Goldman M, Hildebrand J, Brotchi J. Intracerebral transplantation of fetal ventral mesencephalon for patients with advanced Parkinson's disease. Methodology and 6-month to 1-year follow-up in 3 patients. Stereotact Funct Neurosurg. 1997;69(1–4 Pt 2): 99–111.
21. Wenning GK, Odin P, Morrish P, Rehncrona S, Widner H, Brundin P, Rothwell JC, Brown R, Gustavii B, Hagell P, Jahanshahi M, Sawle G, Bjorklund A, Brooks DJ, Marsden CD, Quinn NP, Lindvall O. Short- and long-term survival and function of unilateral intrastriatal dopaminergic grafts in Parkinson's disease. Ann Neurol. 1997;42(1):95–107.
22. Hagell P, Schrag A, Piccini P, Jahanshahi M, Brown R, Rehncrona S, Widner H, Brundin P, Rothwell JC, Odin P, Wenning GK, Morrish P, Gustavii B, Bjorklund A, Brooks DJ, Marsden CD, Quinn NP, Lindvall O. Sequential bilateral transplantation in Parkinson's disease: Effects of the second graft. Brain 1999;122 (Pt 6):1121–32.
23. Mendez I, Dagher A, Hong M, Gaudet P, Weerasinghe S, McAlister V, King D, Desrosiers J, Darvesh S, Acorn T, Robertson H. Simultaneous intrastriatal and intranigral fetal dopaminergic grafts in patients with Parkinson disease: A pilot study. Report of three cases. J Neurosurg. 2002;96(3):589–96.
24. Madrazo I, Leon V, Torres C, Aguilera MC, Varela G, Alvarez F, Fraga A, Drucker-Colin R, Ostrosky F, Skurovich M. Transplantation of fetal substantia nigra and adrenal medulla to the caudate nucleus in two patients with Parkinson's disease. N Engl J Med. 1988;318(1):51.
25. Freed CR, Greene PE, Breeze RE, Tsai WY, DuMouchel W, Kao R, Dillon S, Winfield H, Culver S, Trojanowski JQ, Eidelberg D, Fahn S. Transplantation of embryonic dopamine neurons for severe Parkinson's disease. N Engl J Med. 2001;344(10):710–9.
26. Hauser RA, Freeman TB, Snow BJ, Nauert M, Gauger L, Kordower JH, Olanow CW. Long-term evaluation of bilateral fetal nigral transplantation in Parkinson disease. Arch Neurol. 1999;56(2):179–87.
27. Kordower JH, Freeman TB, Chen EY, Mufson EJ, Sanberg PR, Hauser RA, Snow B, Olanow CW. Fetal nigral grafts survive and mediate clinical benefit in a patient with Parkinson's disease. Mov Disord. 1998;13(3):383–93.
28. Piccini P, Lindvall O, Bjorklund A, Brundin P, Hagell P, Ceravolo R, Oertel W, Quinn N, Samuel M, Rehncrona S, Widner H, Brooks DJ. Delayed recovery of movement-related cortical function in Parkinson's disease after striatal dopaminergic grafts. Ann Neurol. 2000;48(5):689–95.
29. Piccini P, Brooks DJ, Bjorklund A, Gunn RN, Grasby PM, Rimoldi O, Brundin P, Hagell P, Rehncrona S, Widner H, Lindvall O. Dopamine release from nigral transplants visualized in vivo in a Parkinson's patient. Nat Neurosci. 1999;2(12):1137–40.
30. Olanow CW, Goetz CG, Kordower JH, Stoessl AJ, Sossi V, Brin MF, Shannon KM, Nauert GM, Perl DP, Godbold J, Freeman TB. A double-blind controlled trial of bilateral fetal nigral transplantation in Parkinson's disease. Ann Neurol. 2003;54(3):403–14.
31. Kefalopoulou Z, Politis M, Piccini P, Mencacci N, Bhatia K, Jahanshahi M, Widner H, Rehncrona S, Brundin P, Bjorklund A, Lindvall O, Limousin P, Quinn N, Foltynie T. Long-term clinical outcome of fetal cell transplantation for Parkinson disease: Two case reports. JAMA Neurol. 2014;71(1):83–7.
32. Hallett PJ, Cooper O, Sadi D, Robertson H, Mendez I, Isacson O. Long-term health of dopaminergic neuron transplants in Parkinson's disease patients. Cell Rep. 2014; 7(6):1755–61.
33. Ma Y, Tang C, Chaly T, Greene P, Breeze R, Fahn S, Freed C, Dhawan V, Eidelberg D. Dopamine cell implantation in Parkinson's disease: Long-term clinical and (18)F-FDOPA PET outcomes. J Nucl Med. 2010;51(1): 7–15.
34. Kriks S, Shim JW, Piao J, Ganat YM, Wakeman DR, Xie Z, Carrillo-Reid L, Auyeung G, Antonacci C, Buch A, Yang L, Beal MF, Surmeier DJ, Kordower JH, Tabar V, Studer L. Dopamine neurons derived from human ES cells efficiently engraft in animal models of Parkinson's disease. Nature 2011;480(7378):547–51.
35. Cooper O, Hargus G, Deleidi M, Blak A, Osborn T, Marlow E, Lee K, Levy A, Perez-Torres E, Yow A, Isacson O. Differentiation of human ES and Parkinson's disease iPS cells into ventral midbrain dopaminergic neurons requires a high activity form of SHH, FGF8a and specific regionalization by retinoic acid. Mol Cell Neurosci. 2010;45(3):258–66.
36. Ganat YM, Calder EL, Kriks S, Nelander J, Tu EY, Jia F, Battista D, Harrison N, Parmar M, Tomishima MJ, Rutishauser U, Studer L. Identification of embryonic stem cell-derived midbrain dopaminergic neurons for engraftment. J Clin Invest. 2012;122(8):2928–39.
37. Grealish S, Diguet E, Kirkeby A, Mattsson B, Heuer A, Bramoulle Y, Van Camp N, Perrier AL, Hantraye P, Bjorklund A, Parmar M. Human ESC-derived dopamine neurons show similar preclinical efficacy and potency to fetal neurons when grafted in a rat model of Parkinson's disease. Cell Stem Cell 2014;15(5):653–65.
38. Revazova ES, Turovets NA, Kochetkova OD, Kindarova LB, Kuzmichev LN, Janus JD, Pryzhkova MV. Patient-specific stem cell lines derived from human parthenogenetic blastocysts. Cloning Stem Cells 2007;9(3):432–49.
39. Revazova ES, Turovets NA, Kochetkova OD, Agapova LS, Sebastian JL, Pryzhkova MV, Smolnikova VI, Kuzmichev LN, Janus JD. HLA homozygous stem cell lines derived from human parthenogenetic blastocysts. Cloning Stem Cells 2008;10(1):11–24.

40. Isaev DA, Garitaonandia I, Abramihina TV, Zogovic-Kapsalis T, West RA, Semechkin AY, Muller AM, Semechkin RA. In vitro differentiation of human parthenogenetic stem cells into neural lineages. Regen Med. 2012;7(1):37–45.
41. Turovets N, Fair J, West R, Ostrowska A, Semechkin R, Janus J, Cui L, Agapov V, Turovets I, Semechkin A, Csete M, Agapova L. Derivation of high-purity definitive endoderm from human parthenogenetic stem cells using an in vitro analog of the primitive streak. Cell Transplant. 2012;21(1):217–34.
42. Taylor CJ, Bolton EM, Pocock S, Sharples LD, Pedersen RA, Bradley JA. Banking on human embryonic stem cells: Estimating the number of donor cell lines needed for HLA matching. Lancet 2005;366(9502):2019–25.
43. Gonzalez R, Garitaonandia I, Abramihina T, Wambua GK, Ostrowska A, Brock M, Noskov A, Boscolo FS, Craw JS, Laurent LC, Snyder EY, Semechkin RA. Deriving dopaminergic neurons for clinical use. A practical approach. Sci Rep. 2013;3(1463):1–5.
44. Gonzalez R, Garitaonandia I, Crain A, Poustovoitov M, Abramihina T, Noskov A, Jiang C, Morey R, Laurent LC, Elsworth JD, Snyder EY, Redmond DE Jr, Semechkin R. Proof of concept studies exploring the safety and functional activity of human parthenogenetic-derived neural stem cells for the treatment of Parkinson's disease. Cell Transplant 2015;24(4):681–90.
45. Garitaonandia I, Amir H, Boscolo FS, Wambua GK, Schultheisz HL, Sabatini K, Morey R, Waltz S, Wang YC, Tran H, Leonardo TR, Nazor K, Slavin I, Lynch C, Li Y, Coleman R, Gallego Romero I, Altun G, Reynolds D, Dalton S, Parast M, Loring JF, Laurent LC. Increased risk of genetic and epigenetic instability in human embryonic stem cells associated with specific culture conditions. PLoS One 2015;10(2):e0118307.
46. Laurent LC, Ulitsky I, Slavin I, Tran H, Schork A, Morey R, Lynch C, Harness JV, Lee S, Barrero MJ, Ku S, Martynova M, Semechkin R, Galat V, Gottesfeld J, Izpisua Belmonte JC, Murry C, Keirstead HS, Park HS, Schmidt U, Laslett AL, Muller FJ, Nievergelt CM, Shamir R, Loring JF. Dynamic changes in the copy number of pluripotency and cell proliferation genes in human ESCs and iPSCs during reprogramming and time in culture. Cell Stem Cell 2011;8(1):106–18.
47. Elsworth JD, Deutch AY, Redmond DE Jr, Taylor JR, Sladek JR Jr, Roth RH. Symptomatic and asymptomatic 1-methyl-4-phenyl-1,2,3,6-tetrahydropyridine-treated primates: Biochemical changes in striatal regions. Neuroscience 1989; 33(2):323–31.
48. Elsworth JD, Taylor JR, Sladek JR Jr, Collier TJ, Redmond DE Jr, Roth RH. Striatal dopaminergic correlates of stable parkinsonism and degree of recovery in old-world primates one year after MPTP treatment. Neuroscience 2000;95(2):399–408.
49. Redmond DE Jr. Behavioral assessment in the African green monkey after MPTP administration. In: Lane EL, Dunnett SB, editors. Animal models of movement disorders volume I. Neuromethods. Springer Science; 2011. p. 401–35.
50. Taylor JR, Lawrence MS, Redmond DE Jr, Elsworth JD, Roth RH, Nichols DE, Mailman RB. Dihydrexidine, a full dopamine D1 agonist, reduces MPTP-induced parkinsonism in monkeys. Eur J Pharmacol. 1991;199(3):389–91.
51. Taylor JR, Elsworth JD, Roth RH, Sladek JR Jr, Redmond DE Jr. Severe long-term 1-methyl-4-phenyl-1,2,3,6-tetrahydropyridine-induced parkinsonism in the vervet monkey (Cercopithecus aethiops sabaeus). Neuroscience 1997;81(3):745–55.
52. Baulu J, Redmond DE Jr. Social and nonsocial behaviours of sex- and age-matched enclosed and free-ranging rhesus monkeys (Macaca mulatta). Folia Primatol (Basel) 1980;34(3–4):239–58.
53. Redmond DE Jr, Sladek JR Jr, Roth RH, Collier TJ, Elsworth JD, Deutch AY, Haber S. Fetal neuronal grafts in monkeys given methylphenyltetrahydropyridine. Lancet 1986;1(8490):1125–7.
54. Redmond DE Jr, Bjugstad KB, Teng YD, Ourednik V, Ourednik J, Wakeman DR, Parsons XH, Gonzalez R, Blanchard BC, Kim SU, Gu Z, Lipton SA, Markakis EA, Roth RH, Elsworth JD, Sladek JR Jr, Sidman RL, Snyder EY. Behavioral improvement in a primate Parkinson's model is associated with multiple homeostatic effects of human neural stem cells. Proc Natl Acad Sci USA 2007;104(29):12175–80.
55. Redmond DE Jr, Vinuela A, Kordower JH, Isacson O. Influence of cell preparation and target location on the behavioral recovery after striatal transplantation of fetal dopaminergic neurons in a primate model of Parkinson's disease. Neurobiol Dis. 2008;29(1):103–16.
56. Elsworth JD, Sladek JR Jr, Taylor JR, Collier TJ, Redmond DE Jr, Roth RH. Early gestational mesencephalon grafts, but not later gestational mesencephalon, cerebellum or sham grafts, increase dopamine in caudate nucleus of MPTP-treated monkeys. Neuroscience 1996;72(2):477–84.
57. Morrow BA, Roth RH, Redmond DE Jr, Elsworth JD. Impact of methamphetamine on dopamine neurons in primates is dependent on age: Implications for development of Parkinson's disease. Neuroscience 2011;189:277–85.
58. West MJ, Slomianka L, Gundersen HJ. Unbiased stereological estimation of the total number of neurons in the subdivisions of the rat hippocampus using the optical fractionator. Anat Rec. 1991;231(4):482–97.
59. Dorph-Petersen KA, Nyengaard JR, Gundersen HJ. Tissue shrinkage and unbiased stereological estimation of particle number and size. J Microsc. 2001;204(Pt 3):232–46.
60. Ma H, Morey R, O'Neil RC, He Y, Daughtry B, Schultz MD, Hariharan M, Nery JR, Castanon R, Sabatini K, Thiagarajan RD, Tachibana M, Kang E, Tippner-Hedges R, Ahmed R, Gutierrez NM, Van Dyken C, Polat A, Sugawara A, Sparman M, Gokhale S, Amato P, Wolf DP, Ecker JR, Laurent LC, Mitalipov S. Abnormalities in human pluripotent cells due to reprogramming mechanisms. Nature 2014;511(7508):177–83.
61. Love MI, Huber W, Anders S. Moderated estimation of fold change and dispersion for RNA-seq data with DESeq2. Genome Biol. 2014;15(12):550.
62. Huber W, Carey VJ, Gentleman R, Anders S, Carlson M, Carvalho BS, Bravo HC, Davis S, Gatto L, Girke T, Gottardo R, Hahne F, Hansen KD, Irizarry RA, Lawrence M, Love MI, MacDonald J, Obenchain V, Oles AK, Pages H, Reyes A, Shannon P, Smyth GK, Tenenbaum D, Waldron L, Morgan M. Orchestrating high-throughput genomic analysis with bioconductor. Nat Methods 2015;12(2):115–21.
63. Benjamini Y, Hochberg Y. Controlling the false discovery rate: A practical and powerful approach to multiple testing. J R Stat Soc Series B Stat Methodol. 1995;57(1):289–300.
64. Huang DW, Sherman BT, Lempicki RA. Systematic and integrative analysis of large gene lists using DAVID bioinformatics resources. Nat Protoc. 2009;4(1):44–57.

65. Huang DW, Sherman BT, Lempicki RA. Bioinformatics enrichment tools: Paths toward the comprehensive functional analysis of large gene lists. Nucleic Acids Res. 2009;37(1):1–13.
66. Mostafavi S, Ray D, Warde-Farley D, Grouios C, Morris Q. GeneMANIA: A real-time multiple association network integration algorithm for predicting gene function. Genome Biol. 2008;9 Suppl 1:S4.
67. Montojo J, Zuberi K, Rodriguez H, Kazi F, Wright G, Donaldson SL, Morris Q, Bader GD. GeneMANIA Cytoscape plugin: Fast gene function predictions on the desktop. Bioinformatics 2010;26(22):2927–8.
68. Shannon P, Markiel A, Ozier O, Baliga NS, Wang JT, Ramage D, Amin N, Schwikowski B, Ideker T. Cytoscape: A software environment for integrated models of biomolecular interaction networks. Genome Res. 2003;13(11): 2498–504.
69. Smoot ME, Ono K, Ruscheinski J, Wang PL, Ideker T. Cytoscape 2.8: New features for data integration and network visualization. Bioinformatics 2011;27(3):431–2.
70. Xiromerisiou G, Hadjigeorgiou GM, Papadimitriou A, Katsarogiannis E, Gourbali V, Singleton AB. Association between AKT1 gene and Parkinson's disease: A protective haplotype. Neurosci Lett. 2008;436(2):232–4.
71. Ran C, Westerlund M, Anvret A, Willows T, Sydow O, Galter D, Belin AC. Genetic studies of the protein kinase AKT1 in Parkinson's disease. Neurosci Lett. 2011;501(1): 41–4.
72. Hurtado-Lorenzo A, Anand VS. Heat shock protein 90 modulates LRRK2 stability: Potential implications for Parkinson's disease treatment. J Neurosci. 2008;28(27):6757–9.
73. Weihofen A, Ostaszewski B, Minami Y, Selkoe DJ. Pink1 Parkinson mutations, the Cdc37/Hsp90 chaperones and Parkin all influence the maturation or subcellular distribution of Pink1. Hum Mol Genet. 2008;17(4):602–16.
74. Imai Y, Soda M, Hatakeyama S, Akagi T, Hashikawa T, Nakayama KI, Takahashi R. CHIP is associated with Parkin, a gene responsible for familial Parkinson's disease, and enhances its ubiquitin ligase activity. Mol Cell 2002;10(1):55–67.
75. Dong Z, Wolfer DP, Lipp HP, Bueler H. Hsp70 gene transfer by adeno-associated virus inhibits MPTP-induced nigrostriatal degeneration in the mouse model of Parkinson disease. Mol Ther. 2005;11(1):80–8.
76. Gao X, Carroni M, Nussbaum-Krammer C, Mogk A, Nillegoda NB, Szlachcic A, Guilbride DL, Saibil HR, Mayer MP, Bukau B. Human Hsp70 disaggregase reverses Parkinson's-linked alpha-synuclein amyloid fibrils. Mol Cell 2015;59(5):781–93.
77. Pastukhov YF, Plaksina DV, Lapshina KV, Guzhova IV, Ekimova IV. Exogenous protein HSP70 blocks neurodegeneration in the rat model of the clinical stage of Parkinson's disease. Dokl Biol Sci. 2014;457(1):225–7.
78. Mendez I, Sanchez-Pernaute R, Cooper O, Vinuela A, Ferrari D, Bjorklund L, Dagher A, Isacson O. Cell type analysis of functional fetal dopamine cell suspension transplants in the striatum and substantia nigra of patients with Parkinson's disease. Brain 2005;128(Pt 7):1498–510.
79. Mendez I, Vinuela A, Astradsson A, Mukhida K, Hallett P, Robertson H, Tierney T, Holness R, Dagher A, Trojanowski JQ, Isacson O. Dopamine neurons implanted into people with Parkinson's disease survive without pathology for 14 years. Nat Med. 2008;14(5):507–9.
80. Peterson SE, Loring JF. Genomic instability in pluripotent stem cells: Implications for clinical applications. J Biol Chem. 2014;289(8):4578–84.
81. Sahni R, Weinberger J. Management of intracerebral hemorrhage. Vasc Health Risk Manag. 2007;3(5):701–9.
82. Bergman H, Wichmann T, DeLong MR. Reversal of experimental parkinsonism by lesions of the subthalamic nucleus. Science 1990;249(4975):1436–8.
83. Zhou FC, Bledsoe S, Murphy J. Serotonergic sprouting is induced by dopamine-lesion in substantia nigra of adult rat brain. Brain Res. 1991;556(1):108–16.
84. Deller T, Haas CA, Freiman TM, Phinney A, Jucker M, Frotscher M. Lesion-induced axonal sprouting in the central nervous system. Adv Exp Med Biol. 2006;557:101–21.
85. Nudo RJ. Recovery after brain injury: Mechanisms and principles. Front Hum Neurosci. 2013;7:887.
86. Hallett PJ, Deleidi M, Astradsson A, Smith GA, Cooper O, Osborn TM, Sundberg M, Moore MA, Perez-Torres E, Brownell AL, Schumacher JM, Spealman RD, Isacson O. Successful function of autologous iPSC-derived dopamine neurons following transplantation in a non-human primate model of Parkinson's disease. Cell Stem Cell 2015;16(3): 269–74.
87. Bernheimer H, Birkmayer W, Hornykiewicz O, Jellinger K, Seitelberger F. Brain dopamine and the syndromes of Parkinson and Huntington. Clinical, morphological and neurochemical correlations. J Neurol Sci. 1973;20(4):415–55.
88. Pakkenberg H, Andersen BB, Burns RS, Pakkenberg B. A stereological study of substantia nigra in young and old rhesus monkeys. Brain Res. 1995;693(1–2):201–6.
89. Lindvall O. Developing dopaminergic cell therapy for Parkinson's disease—Give up or move forward? Mov Disord. 2013;28(3):268–73.
90. Rudow G, O'Brien R, Savonenko AV, Resnick SM, Zonderman AB, Pletnikova O, Marsh L, Dawson TM, Crain BJ, West MJ, Troncoso JC. Morphometry of the human substantia nigra in ageing and Parkinson's disease. Acta Neuropathol. 2008;115(4):461–70.
91. Bjugstad KB, Teng YD, Redmond DE Jr, Elsworth JD, Roth RH, Cornelius SK, Snyder EY, Sladek JR Jr. Human neural stem cells migrate along the nigrostriatal pathway in a primate model of Parkinson's disease. Exp Neurol. 2008;211(2):362–9.
92. Wakeman DR, Redmond DE Jr, Dodiya HB, Sladek JR Jr, Leranth C, Teng YD, Samulski RJ, Snyder EY. Human neural stem cells survive long term in the midbrain of dopamine-depleted monkeys after GDNF overexpression and project neurites toward an appropriate target. Stem Cells Transl Med. 2014;3(6):692–701.
93. Doi D, Samata B, Katsukawa M, Kikuchi T, Morizane A, Ono Y, Sekiguchi K, Nakagawa M, Parmar M, Takahashi J. Isolation of human induced pluripotent stem cell-derived dopaminergic progenitors by cell sorting for successful transplantation. Stem Cell Reports 2014;2(3):337–50.
94. Peng J, Liu Q, Rao MS, Zeng X. Survival and engraftment of dopaminergic neurons manufactured by a good manufacturing practice-compatible process. Cytotherapy 2014;16(9):1305–12.
95. Moore SF, Guzman NV, Mason SL, Williams-Gray CH, Barker RA. Which patients with Parkinson's disease participate in clinical trials? One centre's experiences with a new cell based therapy trial (TRANSEURO). J Parkinsons Dis. 2014;4(4):671–6.